TOPICAL REVIEW

On erosion issues associated with the leading edge of wind turbine blades

M H Keegan[1], D H Nash[2] and M M Stack[2]

1 Wind Energy Systems CDT, University of Strathclyde, Glasgow, UK
2 Mechanical and Aerospace Engineering, University of Strathclyde, Glasgow, UK

E-mail: mark.h.keegan@strath.ac.uk

Abstract

The increasing developments in wind turbine technology, coupled with an unpredictable operating environment, presents significant challenges regarding erosion issues on the leading edge of the blade tips. This review examines the potential degradation posed by the different environmental variables, with specific emphasis on both rain droplet and hailstone impact on the blade leading edge. Drawing on both the insights from experimental results and recent field data from the literature, the mechanisms of leading edge erosion are discussed. Meteorological tools that may enable rain and hailstone erosion prediction are addressed as well as potential experimental and numerical approaches that may provide insight into the nature of impact and erosion on the blade surface.

1. Introduction

Innovation in sustainable energy sources has ensured that the demand for installed wind capacity has increased rapidly in the last decade. In the year 2000, the total capacity of installed wind in the EU stood at 12.9GW. This grew over the next decade to 106GW by the year 2012; with 10% of this total comprising of offshore capacity [1]. The European Wind Energy Association (EWEA) [2] has also targeted further growth to 230GW by the year 2020, with 40GW comprising of offshore installations, representing an unprecedented growth in a relatively new form of wind turbine operation.

Due to factors such as site wind resource and planning constraints, many wind farms are located in relatively challenging operating environments such as exposed or hilly terrain where inclement weather conditions – which may be desirable for wind resource - may commonly be expected, or alternatively in offshore locations where the turbine is fully exposed to the elements. As such, many wind turbines will be exposed to a variety of environmental and tribological effects over their operational lifetimes. These include: extreme wind/gusts, frequent rain showers, hailstone showers, snow, icing, extremes temperatures and ultraviolet light exposure (UV). Hence, the operational behaviour and the vast scale of modern wind turbine designs, coupled with these environmental factors, presents significant engineering challenges. This is particularly the case at the leading edge of the blade tips where the significant tip speeds exhibited in modern designs - commonly now greater than $80ms^{-1}$ - can lead to significant erosion, as will be discussed below.

The following review evaluates for wind turbine blades, the prominent types of environmental exposure, the nature of their interaction with the blade leading edge and the robustness of leading edge material technologies, in order to better define the issue of leading edge erosion and impact damage.

2. Utility scale wind turbine design & operation

As a consequence of the requirement in increased energy capture for utility scale wind turbines, the scope and scale of modern wind turbine blade technology has undergone rapid growth. Figure 1, shows the growth trends in blade length and rated power for utility scale wind turbines over nearly three decades.
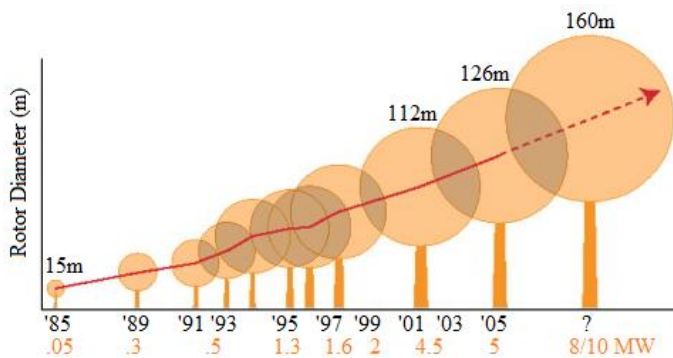
Figure 1. Blade length and rated power trends for wind turbines. Source: **[3]**

This increase in blade length coupled with the operational procedure of modern turbine designs has resulted in an increase in the blade tip speeds exhibited by many designs. Figure 2 plots the maximum blade tip speed against the associated rotor diameter for numerous utility scale turbines from various manufacturers.
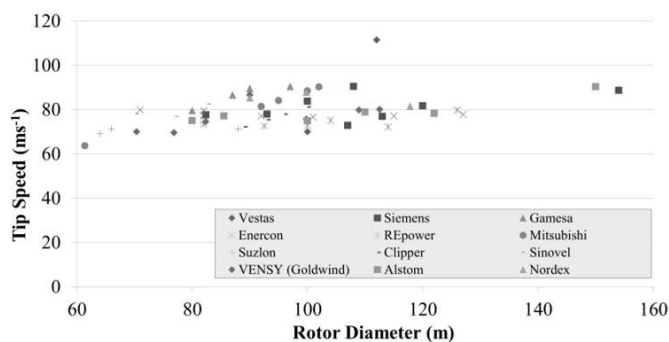

Figure 2. Blade tip speed vs. rotor diameter for various utility scale wind turbine models. Data sourced from numerous manufacturer literature.

As shown, tip speeds in excess of $80ms^{-1}$ are now commonplace for large wind turbine designs, and from the data, it would appear that there is a slight trend in increasing tip speed with increasing rotor diameter; however the tip speed will also be heavily dependent on turbine operational strategy and control. Furthermore, when considering the impact of rain, hailstones and other particulates on the leading edge, the incoming velocity of the projectile may also play a role in the potential impact velocities.

It should also be pointed out that these tip speeds only represent the maximum possible values for the given design. During their operational lifetimes, the turbines may only operate at these speeds for a limited (but significant) amount of time.

Indeed, it is important to note not only the magnitude of the tip speeds exhibited by the blades, but also the total amount of operational hours the blade will complete in its lifetime. A typical wind turbine may be expected to operate continuously for approximately 15 years over its service life (this is of course site and design sensitive), the significance of this duration is highlighted further when considering that most modern automobiles may only ever operate continuously for around 9 months [4]. During these years of continual operation, the materials of the blade are not only exposed to varied environmental factors, but are also subject to constant fatigue loading. Additionally, during this period, the frequency of maintenance and access to the blade has to be kept to minimum in order to reduce the production and financial losses associated with turbine down time.

3. Blade materials

The large and ever-growing scale of modern wind turbine blades has resulted in the widespread implementation of fiber reinforced plastic composite material technologies in blade designs. Such composite technologies can boast high specific strength and stiffness properties (ideal for long slender load bearing structures). Additionally, composites can exhibit excellent fatigue properties when compared to other high performance alloys.

Most modern blade designs utilise composites which feature a thermosetting polymer matrix, such as epoxy or polyester, with reinforcing glass or carbon fibers. The configuration in which these constituents are combined and applied can be altered and varied to match the design requirements for certain areas of the blade [5] [6] . For instance, thin sectioned areas of the blade may comprise of laminates consisting of multiple and variably orientated unidirectionally reinforced plies, whereas in thicker or more structurally critical areas a laminate consisting of biaxial or triaxial weave reinforced plies may be employed. Most large designs also feature the application of section thickening sandwich materials such as balsa wood or polymer foams, to add thickness to sections which may otherwise be prone to buckling (trailing edge, central spar etc.) [7].

Although the composite material technologies employed boast many advantageous characteristics, they also have some inherent weaknesses and drawbacks, such as

performing poorly under transverse impact (i.e. perpendicular to the reinforcement direction) and being sensitive to environmental factors such as heat, moisture, salinity and UV; as will be discussed. To address these weaknesses and environmental sensitivities, a great deal of effort is invested by blade manufacturers and blade material manufacturers in creating effective protective surface coatings [8] [9] [10]. The main purposes of such protective coating systems are as follows:

1. To act as a barrier from environmental factors such as UV and moisture which can affect the material properties of the composite structure
2. Protect the composite substrate from foreign body impact, whether that is during manufacture and handling, installation & maintenance or from rain, hailstone and other forms of impact during operation.

The technologies employed vary widely, however the two most common approaches to creating an effective surface coating are:

1. **In-mould Application** – A surface coating layer is added to the surface of the blade as part of the moulding process. For manufacturing reasons, the coatings created through this approach typically consist of a layer of material similar to that of the matrix material used in the substrate (e.g. epoxy/polyester)
2. **Post-mould Application** – Surface coatings can be applied to the blade after the moulding process through painting or spraying. This approach allows more flexibility with regards to material choice (in the absence of moulding considerations), with some manufacturers choosing to apply more ductile/elastic material components such as polyurethanes. [11]

It is of course possible to combine these techniques to provide a satisfactory surface coating solution and many manufacturers do. However, the process executed and materials utilised by manufacturers are often proprietary matters and are therefore not always fully disclosed. In addition to this, there is also a certain degree of ambiguity around the terminology of surface coating technologies for wind turbine blades, whereby the surface coating - irrespective of material choice or application method - is referred to as a 'gelcoat'. In addition to the gelcoat, some operators may also decide to implement a leading edge tape product, manufactured by material companies such as 3M [12]. These technologies usually consist of a highly elastic and durable polyurethane material, designed to (in some cases sacrificially) absorb the impact energy from airborne particulates.

In the region of the leading edge at the blade tip, a cross section of most utility scale wind turbines would reveal several layers of the main structural composite material (i.e. epoxy/glass fiber), some larger designs may also incorporate thickening sandwich materials (such as balsa wood or low density foams). These components represent the main structural constituent of the skin cross section [7]. Above these layers, the respective protective coating system would be evident. This may comprise of one single layer of gelcoat material or indeed several individually purposed layers. For instance, separate coating technologies can be applied to protect against different environmental threats, such as a special UV resistant gel coat or a layer of randomly orientated chopped strand mat polymer composite to create additional impact protection. The precise configuration and material selection varies greatly between manufacturers and designs, however, the fundamental layup at the leading edge of the blade tip region will consist of the structural layup with a protection coating system.

4. Leading edge erosion in literature

Detailed and thoroughly documented examples of leading edge erosion on wind turbine blades are sparsely available in the publicly available literature. However, it is generally agreed that leading edge erosion is an important challenge for manufacturers and operators. Wood [13] states that some operators have found that leading edge erosion can become an issue after only two years of turbine operation; much sooner than expected. This early onset of energy capture altering leading edge erosion has prompted some manufacturers to begin to address the issue in the design stage through exploring new protective coating options. Wood [13] also draws on the experiences of operators, manufacturers and inspection & repair companies to emphasize the need for effective inspection & maintenance to ensure satisfactory performance of the blade throughout its service life. In the early years of the North American wind industry,

Rempel [14] states there was an expectation that once blades were in operation, routine inspection and maintenance would not be necessary. As the industry matured it became clear that the issue of leading edge erosion was significant and that maintenance would be essential if the blades were to reach their expected design life. Rempel [14] also explains that careful handling of the blade during manufacture, transport and installation is also essential to avoid small tears or scratches which may act as initiation sites for further wear and erosion. Rempel [14] states that leading edge erosion on an unprotected blade, based on observations in the field, may occur after only three years, with the tip being most susceptible to wear, but with erosion also exhibited on the more inboard portions of the blade.

The issue of leading edge erosion is cited as a concern by numerous service & repair companies [15] [16] [17] [18] and although these sources and the previous two articles cited [13] [14] are based mostly on anecdotal accounts, the wealth of references to the issue and the supporting images given, such as that in figure 3, emphasize the real dangers posed by erosion to the leading edge.

Figure 3. Example of leading edge erosion. Source: [14]

A significant issue with the sources discussed is that they seldom give any real detail on the cause or mechanisms of damage. They therefore do not shed a great deal of light on the main causes of leading edge erosion, nor the way in which the process evolves and progresses.

Dalili et al. [19] investigated a wide range of surface engineering issues in relation to the performance of wind turbine blades, focussing primarily however, on the problems presented by icing in Nordic climates. They state that particle or droplet laden winds can erode the leading edge of the wind turbine blade and for some aerofoils this may lead to a reduction in the aerodynamic efficiency of the blade. Methods of improving blade

erosion resistance are also discussed, highlighting the proposed benefits of applying elastometric materials to the leading edge (i.e. leading edge tapes), but also stating that tapes must be replaced frequently as they become worn. Innovations in materials and design, with a view to improving erosion resistance are also discussed, making reference to the development of large thermoplastic based composite blade designs which would in theory provide superior impact and erosive resistance [20]. The development of adding nano-sized reinforcement to elastomers to create a new nanocomposite material for leading edge application is also detailed. In a similar field of nano research, Karmouch and Ross [21] propose a method of embedding silica nanoparticles in an epoxy paint to act as a hydrophobic barrier on wind turbine blade surfaces. They have found that this simple method creates a water repellent surface, forcing water to run off. There is little discussion however with regard to how these surfaces would perform with respect to erosion.

Sayer et al. [22] detailed an investigation of the material properties of an 11.6m length DEBRA-25 wind turbine blade (100kW rating), after having completed almost 20 years of operation. They note in the concluding statements that there was significant evidence of rain erosion effects exhibited at the blade tips. The tip speed of the DEBRA-25 is stated as being $65.4ms^{-1}$ [23], which is comparatively low compared to that of modern, larger scale turbines, as shown in figure 2. The region of operation in southern Germany is also relatively dry compared to many other regions in Europe (figure 10). Given this comparatively low tip speed and dry climate, it is interesting to note that rain erosion at the blade tips was still a significant issue.

As part of an effort to address the issue of leading edge erosion, many blade manufacturers are researching and developing new material systems for their blade leading edges. Haag [11] detailed the development process behind the creation a new advanced coating technology for LM Wind blades, named ProBlade™, in a presentation at the European Wind Energy Conference, 2013. The technology, developed in partnership with their suppliers, comprises of a "highly flexible 2-component solvent free UV-resistant polyurethane based paint" and was developed to improve the erosion performance of blades with Polyester based substrates. It offers minimum aerodynamic influence and less noise

generation than tape. Haag [11] detailed the extent of the damage created on the leading edge of a blade sample, protected only by a typical Polyester gelcoat, after being subjected to 30-35mm/h simulated rain at 123-157ms^{-1} (varying along the sample length)for 60 minutes. The testing was conducted through use of swirling arm rain erosion apparatus (resulting in the variation in test parameters along the sample length), performed by Polytech [24].
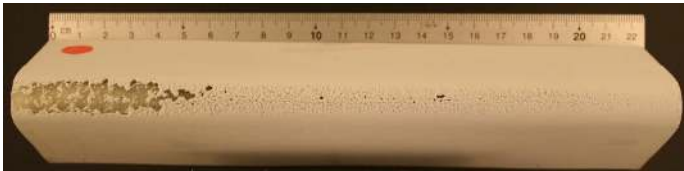

Figure 4. Blade sample with polyester gelcoat, tested at 123-157ms^{-1}, 30-35mm/h simulated rain for 60 minutes. Source: [11]

The sample shown, exhibits a significant amount of leading edge erosion of the Polyester gelcoat, exposing the composite substrate below. Although brought about through an accelerated process, the damage created highlights the potentially harmful effects of rain induced leading edge erosion on wind turbine blades. It is also interesting to note that although 150ms^{-1} is an extreme impact velocity, given the scale and tip speeds of modern blade designs and the nature of rain impact (as will be discussed), it is not far removed from a realistically feasible impact velocity value of about 90-100ms^{-1}. The effectiveness of the ProBlade™ technology is compared to that of a leading edge tape, as shown in figure 5.
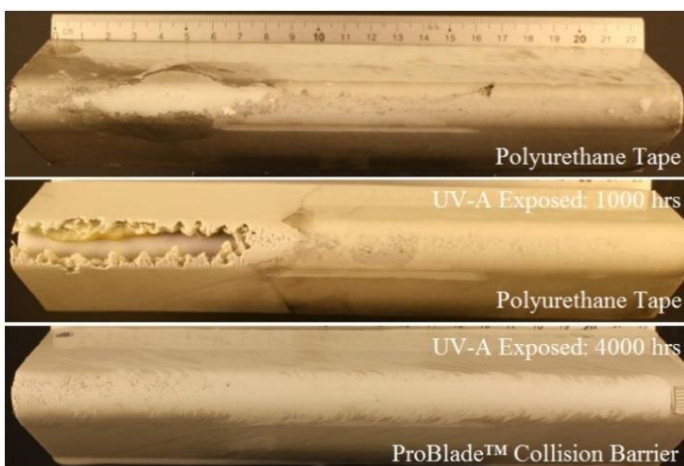

Figure 5. Samples tested under liquid droplet impact at 123-50ms^{-1} at 30-35mm/h for 6 hours. Top-to-bottom: polyurethane tape protection – no UV-A exposure, polyurethane tape - 1000hrs of UV-A exposure and ProBlade™ Collision Barrier protection with 4000hrs of UV-A exposure. Source: [11]

As shown, after 6 hours of rain erosion testing at 150ms^{-1} with a rain rate of 30mm/h, the ProBlade™ coating system successfully resisted any significant erosion effects. In the absence of any UV-A exposure, the polyurethane tape also successfully provided sacrificial protection to the leading edge, however the degradation of the tape would result in the requirement for replacement; therefore potentially proving less cost efficient. It would appear that the ProBlade™ coating delivers further advantages with regards to UV-A exposure when compared to a standard polyurethane tape, as from inspecting the middle sample, it is clear that the introduction of UV-A exposure to the polyurethane tape protected sample resulted in significant leading edge degradation. Whereas, even with 4 times the exposure duration the ProBlade™ system shows very little evidence of significant erosion.

As well as manufacturing leading edge tapes [12], 3M have also developed a coating technology for wind turbine applications, named W4600 [8]; designed to protect against leading edge erosion. Powell [25] showed the effects that leading edge erosion can have over several years of operation, as shown in figure 6.

Figure 6. Examples of leading edge erosion in the field across a range of years in service. Source: **[25]**

As shown, after only one year in service, leading edge erosion may become an issue, with evidence of significant leading erosion exhibited after 10 years in service. As part of their product development and analysis, 3M have also conducted rain erosion testing of samples with and without their coating technologies [25]. Figure 7 shows the results of their rain erosion testing, featuring samples protected by both leading edge tape and an early prototype surface coating [8], comparing them against the results of competitive coating technologies. The testing was conducted at the Rain

Erosion Test Facility at the University of Dayton Research Institute [26] (discussed in more depth later), at an impact velocity of 134ms^{-1}.
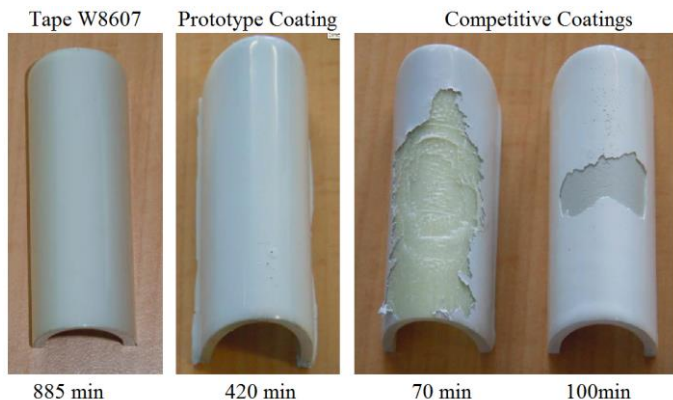

Figure 7. 3M results from rain erosion testing at 134ms^{-1}, for samples protected by: leading edge tape, a prototype surface coating and competitor coatings. Source: **[25]**

As shown, the protective technologies were deemed successful in preventing leading edge erosion, when compared to competitor technologies. Significant leading edge erosion can be observed on the samples protected by competitive coatings, highlighting the potentially extremely damaging effects of rain erosion on blades with sub-standard protection. The further damaging effects of rain erosion of the composite substrate (following the removal of the coating) are also visible, with numerous layers of the composite substrate stripped away in one of the samples with a 'competitive coating'.

Although the test results shown by both Haag [11] and Powell [25] are not examples of erosion occurring in operational wind turbines, they do show the potentially significant leading edge damage brought about through only water droplet impact. Here, it is shown that over the lifetime of a blade, a typical gelcoat technology alone will not guarantee protection from leading edge erosion. The results also highlight the effectiveness of applying highly elastic materials such as polyurethane to the leading edge, in order to absorb the impact energy imposed by rain droplet impact. The importance of considering the damaging effects of multiple environmental factors acting together, such as rain and UV exposure, is also highlighted.

The literature review and studies discussed represent the most prominent research on the specific area of wind turbine leading edge erosion damage. However, a great deal of work has been has been historically conducted to investigate the effects of liquid and particulate induced erosion on the leading edges of aerospace components such as aircraft wings and helicopter rotors. The similarities between wind turbine leading edge erosion and these phenomena make it possible to review such research in order to further broaden the understanding of leading edge erosion in a wind turbine context.

Weigel [27] discussed the importance of utilising an effective leading edge erosion protection system on helicopter rotor devices as well as describing the creation of an new advanced protection system. In order to select an appropriate leading edge protection material, the study evaluates the protection characteristics of a wide range of materials in relation to parameters such as rain and sand erosion resistance (using the Rain Erosion Test Facility at the University of Dayton Research Institute [26]) as well as performance under hydrolysis, impact, UV exposure and salt fog exposure. Weigel [27] identifies that elastomeric materials, such as polyurethanes, can provide superior resistance to solid particle erosion (such as sand) in comparison to metals, and are only outperformed with regards to rain erosion by metals; as a result of poorer polyurethane performance at direct impact angles

Gohardani [28] provided an in-depth review of erosion aspects in aviation applications, addressing both the fundamental physics of liquid and solid particulate impact as well as the techniques – both experimental and numerical – developed to better understand the phenomena of erosion (both of which will be discussed later in more detail). The review finds that the phenomena of erosion and the efforts to analytically model and understand it using classical approaches can prove complex and highly specialised, and recognises that the introduction of high performance composite materials (as also utilised in wind turbine blades) may further complicate such analytical efforts in future. Gohardani [28] therefore highlights the requirements for both experimental and numerical analysis of the issue in future applications, whilst also recognising the added complexity of numerically modelling the response of advanced composite materials. The complexity of such modelling is further emphasised by Gohardani [28] by identifying the requirements in some cases to model on the microscopic, mesoscopic and macroscopic scales when considering composite matrials.

5. Effect of leading edge erosion on wind turbine performance

In order to understand the significance of leading edge erosion on wind turbine blades, it is important to consider the effects that such erosion will have on the performance and lifetime of the blade, as well as on the performance of the turbine as a whole.

It is apparent that one of the most important characteristics of a wind turbine blade is its aerodynamic performance. If leading edge erosion does occur, then it may pose a threat to this aerodynamic performance as a result of roughening the blade surface. For instance, Dalili [19] states that debris from insects on the blade alone can result in a 50% reduction in the power output of turbines; this would prove a critical blow to the profitability of any wind turbine. However, through careful aerofoil selection, blade design and operational strategy selection, the sensitivity of blades to surface roughness/contamination can be significantly reduced [29]. Sareen et al. [30] found that leading edge erosion on a wind turbine aerofoil can produce significant aerodynamic performance degradation. In the study, DU 96-W-180 aerofoils with varying severity and types of leading edge erosion were tested to evaluate the effects of the erosion on performance, finding that such effects resulted in a large increase in the drag of the aerofoil and an earlier onset of stall (i.e. at lower angles of attack). The results from the study showed an increase in drag of 6-500% due to varying levels of leading edge erosion (light-to-heavy). Further analysis predicted that an 80% increase in drag could lead to approximately a 5% reduction in annual energy production. Additionally, in related research, Chinmay also found that implementing leading edge tapes on such aerofoils resulted in a drag increase ranging from 5-15% - depending on placement and area size - and although this may not result in a measurable difference in annual energy production, research would be required to determine the optimum method of application to minimise any detrimental aerodynamic effects [31].

Additionally, it is possible to examine studies into the effects of erosion on the performance helicopter rotors to draw lessons applicable to wind turbine blades. Calvert et al. [32] utilised a Computational Fluid Dynamics approach (CFD) to study the effects of typical surface deformation (from the impact of sand erosion) on the aerodynamic profile of a NACA 63-414 aerofoil. It was found that the introduction of surface deformation resulted in detrimental effects on the aerodynamic performance of the profile, such as an earlier onset of stall (and therefore reduction in maximum lift), an increase in drag and a reduction in thrust. However, it must be noted that the study considered surface deformation of the upper and lower surfaces of the profile; not the leading edge.

To evaluate the benefits of their leading edge protection products, 3M investigated the effect that leading edge erosion can have on the power output of a wind turbine [25] [33]. Figure 8 shows the calculate Annual Energy Production (AEP) over a period of 5 years, for turbines employing the 3 following leading edge protection configurations:

1. Protected by 3M wind protection tape
2. Unprotected and assuming moderate leading edge erosion
3. Unprotected and assuming worst case erosion.

The value of AEP was calculated by taking into account the aerodynamic effects (evaluated experimentally) of the specific level of erosion (on lift and drag) and the effect this has on energy production; assuming a 1.5MW rated turbine and a capacity factor of 30%.
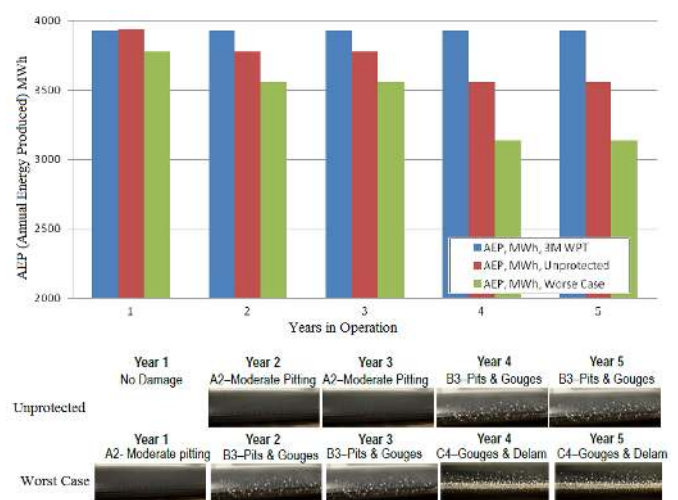

Figure 8. Calculated effects of varying levels of leading edge erosion on the Annual Energy Production of a 1.5MW wind turbine. Source: [25]

From this, it is clear that even moderate levels of leading edge erosion can have a significant effect on the energy output of a wind turbine, with even only moderate pitting

resulting in substantial losses. Such findings further highlight the technology need to establish a more thorough understanding of the issue of leading edge erosion; in order to prevent any potential reductions in both energy capture and consequently profitability.

Reductions in aerodynamic and power efficiency are not the only concern regarding leading edge erosion, as the material integrity of the blade is also an important consideration. As briefly discussed previously, the exposure of the composite substrate to moisture and UV light can have a seriously detrimental effect on its material properties and performance.

The potential effects of UV exposure on the performance of the coating systems was shown in figure 5, however the composite substrate is also based on polymer materials and therefore is also susceptible to the influence of UV exposure. Shokrieh & Bayat [34] showed that through accelerated UV exposure, polyester resin exhibited a decrease of 15% in average failure strain, a decrease of 30% in ultimate strength and an 18% decrease in tensile modulus. When considering a glass fiber reinforced polyester unidirectional composite, under the same exposure, it was found that the shear modulus of the composite decreased by about 20% as a result of such exposure. Kumar et al. [35] showed that UV exposure of a carbon reinforced epoxy composite resulted in the reduction of matrix dominated properties, namely a 29% reduction in transverse tensile strength. These studies show the effects that UV exposure can have on the material properties of the polymer matrix material, with large reductions in material strength exhibited; predominantly in the transverse direction (i.e. the directions in which the fibers do not bear load).

The exposure of the composite substrate to water could also pose significant threats to the performance of the blade. Primarily, the removal of any surface coating will mean that the substrate itself will be exposed to further erosion; as previously exhibited in figure 7. This would have obvious structural implications for the blade, and in the case of through-thickness erosion could result in water and particulate ingress to the internal blade structure. Generally speaking, epoxy resins exhibit good resistance to water degradation, whereas polyester and vinylester are more prone to degradation. A report from the materials manufacturer Gurit [36] states that a thin polyester laminate may retain only 65% of its

interlaminar shear strength following immersion in water for a one year period, whereas, an epoxy laminate may retain around 90%. This effect however, is heavily dependent on the chemical nature of the matrix materials employed, but highlights the possible sensitivities of the matrix and the importance of understanding these.

6. Operational environmental threats

The effects of the environment will inherently vary between site locations and turbine/blade design. It is clear that the main factors which cause leading edge erosion will most likely arise from:

- Exposure to airborne particulates: mainly in the form of rain, hailstone, sea-spray, dust/sand and wild life
- UV light & humidity/moisture

The following sections will review, in depth, the effects of rain and hailstone impact in relation to leading edge erosion. Considerations of other factors such as sea-spray and dust/sand impingement and UV exposure will also be more briefly considered.

7. Rain impact & erosion

7.1 Exposure

As with all environmental factors, the total rainfall a given wind turbine will be exposed to during its lifetime can vary vastly between locations. However, if considering European locations, most sites will be exposed to some level of annual rainfall, and for most it will likely occur more frequently than other forms of precipitation.

Looking specifically at the UK, figure 9 shows a map of the average annual rainfall for the period running from 1981-2010.
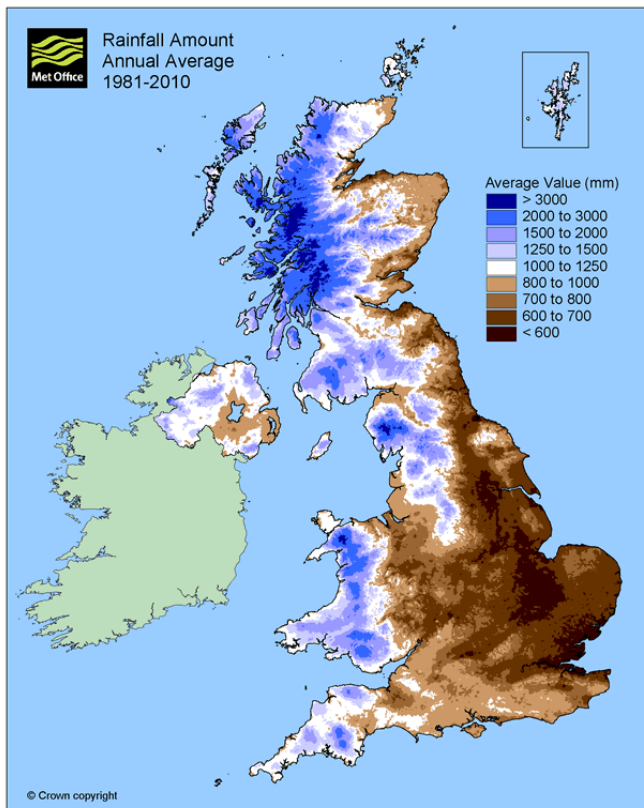
Figure 9. Map of the annual average total rainfall in the UK for the period 1981-2010. Source: **[37]**

From figure 9 it is clear that in the UK the expected level of average annual rainfall varies vastly between different geographical regions. Some areas in the southeast may see less than 600mm of rainfall over an annual period, whereas in the northwest, totals of up to and greater than 3000mm have been observed. Given that the polyester gelcoat protected sample tested and shown in figure 4 was subjected to an approximate rainfall total of 30-35mm over 60 minutes, it is clear that a rainfall amount of 3000mm may be considered significant with regards to rain induced leading edge erosion. Using information such as that shown in figure 9 may then be considered useful when assessing the threat posed by rain erosion for a given site.

It is possible also to examine a wider geographical scale, encompassing most of Europe, as shown in figure 10.
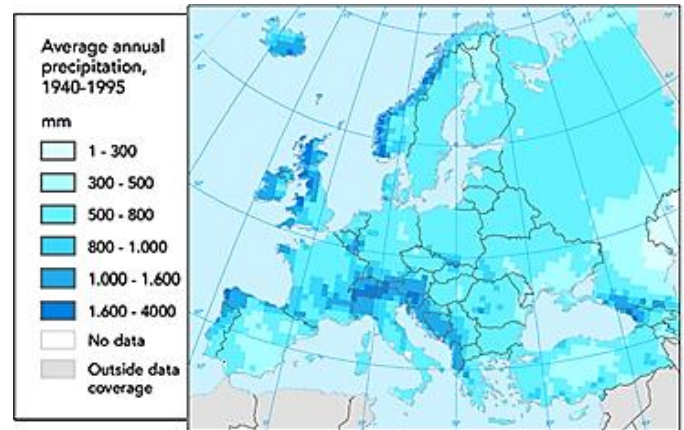

Figure 10. European average annual precipitation for the period of 1940-1995. Original image source: **[38]**

Looking at the precipitation levels in Europe, it is clear that in some mainland areas such as central Spain, Sweden and many eastern European countries, the threat posed by rain induced leading edge erosion may be minimal; as a consequence of very little rainfall. However, in Alpine regions and along the coastline of the Adriatic Sea, the level of rainfall may be considered significant enough that the issue of rain induced leading edge erosion may need to be investigated and designed against. As with the map of the UK, where significant rain fall is observed in the westerly regions, this further highlights the necessity in understanding the potential range of meteorological conditions at any proposed wind turbine site.

7.2 Impact conditions

To understand the nature of rain induced leading edge erosion, the physical nature of rain droplets and their characteristics as a projectile should first be considered.

The diameter of a given raindrop varies with respect to the climatic conditions under which they are formed and the conditions of transport in the air. However, typical raindrop diameters are commonly cited as ranging from 0.5mm to 5mm [40]. At and above this maximum diameter the droplet geometry may become unstable and fragment [41]. Kubilay et al. [42] produced a plot for the probability density for rain droplet diameters, as shown in figure 11, using the equations derived by Best [43].
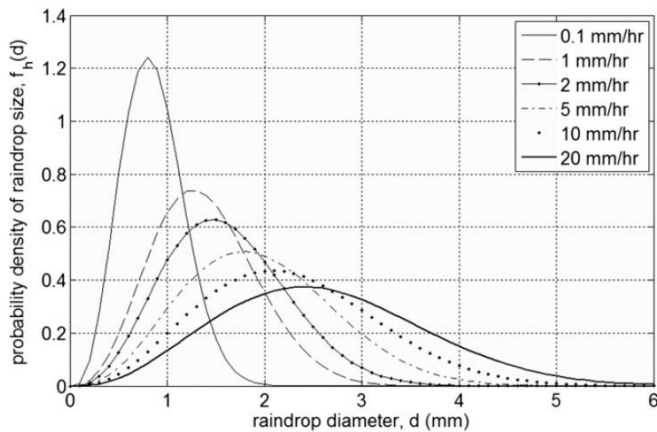
Figure 11. Probability density of raindrop size. Image source: **[42]**. Using equations from: **[43]**

From the probability density plot, it is clear that for mild to moderate rain rates, rain droplet diameters ranging from 0.5-3mm are most common; it is only during more extreme rain rates that droplet diameters in excess of 3mm are exhibited.

The terminal velocity of a falling rain drop is also heavily dependent on the climatic conditions. However, Gunn & Kinzer [44] conducted a measurement campaign to ascertain the terminal free fall velocity of varying water droplet sizes through stagnant air. The results of their findings are shown in figure 12.
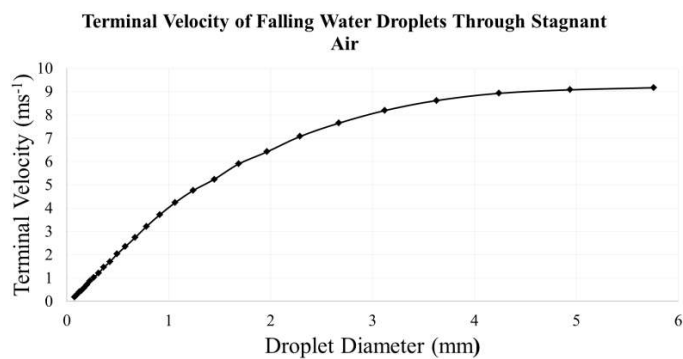

Figure 12. Free fall terminal velocity of water droplets through stagnant air for a range of stable droplet diameters. Data source: **[44]**

From figure 12, it can be seen that the maximum free falling terminal velocity levels out at around 9ms^{-1} for diameters in excess of about 3.5mm.

In the context of wind turbine blade leading edge erosion, the freefalling terminal velocity of the rain droplet plays only a minor role in the magnitude of the impact velocity when compared to the blade tip speeds. It is possible through a process of simple velocity vector calculations to establish an approximate value of potential impact

velocity for given rain and turbine operation conditions; through a whole rotor sweep. For example, taking a rain droplet with a terminal velocity of 8ms^{-1}, fully entrained in a horizontal 20ms^{-1} wind (i.e. assuming that the droplet is also travelling at this speed horizontally), striking a blade with a 90ms^{-1} tangential tip speed (broken down into horizontal and vertical components for calculations), it is possible to calculate the potential impact velocity magnitude for a full rotor sweep. Plotting these calculated potential impact velocity values against their respective rotor position gives the plot shown in figure 13.
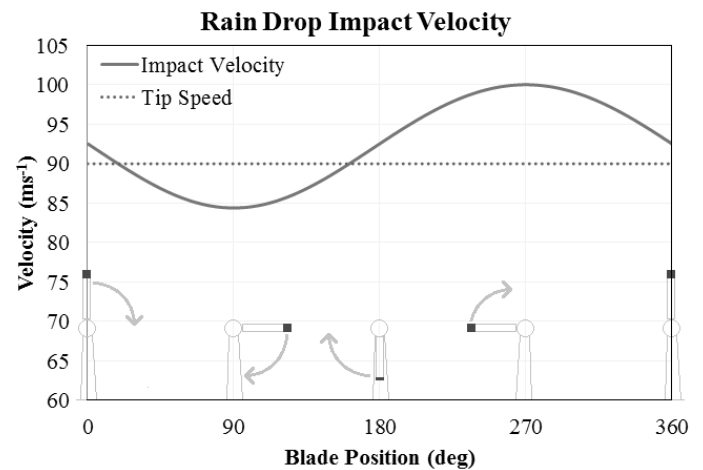

Figure 13. Rain drop impact velocity at the blade tip at positions through a full rotor sweep. Rain drop terminal velocity of 8ms^{-1}, fully entrained in a 20ms^{-1} horizontal wind, striking a blade tip with a 90ms^{-1} tip speed. The tip speed has also been plotted for reference.

Although the values shown in figure 13 are derived from a fairly rudimentary approach that makes some fundamental assumptions, the approach does well to both highlight the potential magnitude of impact velocity values and to act as an aid to understanding the nature of impact on the blade. For instance, it illustrates that even when the blade is rotating in a downward direction (1-179˚ position), as a result of the significant tip speed, the impact velocity between the rain and blade does not drop below 80ms^{-1}; therefore the terminal velocity of the rain acts only to slightly lessen the impact velocity. Conversely, when looking at the impact velocity at the rotor position of 270˚, where the blade and rain drop trajectories are exactly opposed to one another, the additive effects of the terminal velocity to the blade tip velocity can be observed as the peak in the impact velocity.

7.3 Liquid droplet impingement & erosion

The previous section contextualised and quantified the range of possible impact conditions with respect to rain droplet impact on the leading edge of a wind turbine blade. However, it is also important to understand what the magnitudes of these impact velocities mean in the context of liquid droplet impact on a solid surface.

Gohardani [28] displayed the nature of liquid droplet impact on a flat solid surface, as shown in figure 14.
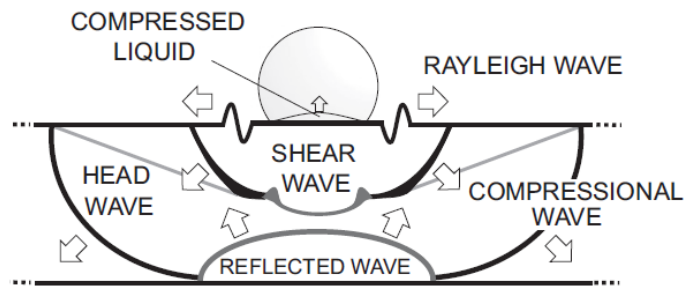

Figure 14. Liquid droplet-solid surface impact interaction, showing shockwave behaviour in both the droplet and target. Source: adapted from **[28]**

It shows the creation of an initial compressional wave in the target material, followed by a shear wave. The interaction of these waves can be complex and will depend upon impact conditions and material properties. A Rayleigh wave, created and confined to the target surface, is also shown. The figure also shows the creation of a compressed liquid wave front in the droplet itself. This behaviour is crucial to understanding the nature of the impact phenomenon, as after a short duration of impact, this upwards compresses liquid wave extends towards and past the contact periphery between the droplet and the surface. After this point lateral jetting (or 'splashing') of the droplet across the surface commences.

To predict the pressure exerted on the surface by the liquid droplet during the initial phases of contact, the waterhammer equation has historically commonly been employed [45]. The waterhammer equation is shown in in equation 1, where P is the waterhammer pressure created during impact, ρ_0 is the undisturbed density of the fluid (water in this case), c_0 is the speed of sound in the undisturbed liquid and V_0 is the impact velocity.

$$P = \rho_0 \, c_0 \, V_0 \qquad (1)$$

This simple equation was first developed to calculate the waterhammer pressure present in piping systems and is therefore based on the following assumptions:

1. The impact is a one dimensional event
2. The target surface is perfectly rigid
3. The water density remains constant during the impact event
4. The speed of sound remains constant during the impact event.

Although these are quite fundamental assumptions, the expression can still be used as a good indicator of the magnitudes of impact pressure that may be expected for a given impact event. Dear & Field [46] proposed a modified waterhammer equation, which takes into consideration not only the propagation of pressure through the liquid during impact, but also the target body; as shown in equation 2, where P is the modified waterhammer pressure imparted during impact, V is the impact velocity, ρ is density, c is the speed of sound, and the subscripts l and s refer to the liquid and solid bodies respectively.

$$P = \frac{V \rho_l c_l \rho_s c_s}{\rho_l c_l + \rho_s c_s} \qquad (2)$$

The expressions shown can be useful in approximating the impact pressure exerted, however they only predict the pressures created during the initial phases of contact. They do not apply to conditions after the onset of droplet lateral jetting across the target surface, when typically the average impact pressure decreases.

An instantaneous approximation of the impact force imparted through liquid droplet impact has also been proposed in previous studies [47] [48], as shown in equation 3, with F representing the impact force, m and d the mass and diameter of the droplet respectively and V, the impact velocity.

$$F = \frac{mV^2}{d} \qquad (3)$$

The force exerted will obviously vary over the duration of the impact event; however this expression again serves as a good tool to approximate the magnitude of impact forces imparted.

It is then worthwhile examining what these expressions can reveal about the magnitudes of the pressures and forces exerted on the blade surface through rain drop impact. Assuming a water density of 1000kgm^{-3} and a speed of sound in water of 1500ms^{-1} [49] for the waterhammer equation (equation 1) and a droplet diameter of 2mm for the instantaneous force equation (equation 3), both expressions can be calculated and plotted against a range of potential impact velocities, as shown in figure 15.
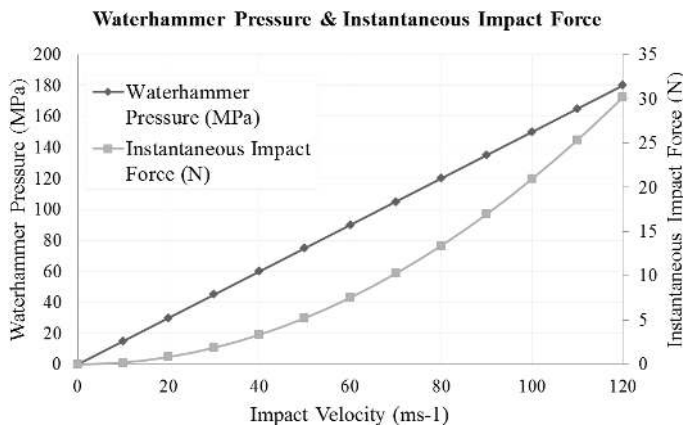

Figure 15. Waterhammer pressure and instantaneous impact force from a 2mm diameter liquid droplet impact over a range of potential impact velocities.

As shown in figure 15, the impact pressures create by a moderately sized 2mm diameter rain drop can be considered significant in the context of leading edge impact. At a common tip speed of around 80ms^{-1} (figure 2) such a droplet could impart up to 120MPa of pressure on the blade surface.

The impact energy is also an important consideration with regards to impact studies and for rain drop impact it is simply equated to the kinetic energy of the impacting droplet (equation 4).

$$KE = \frac{1}{2}mV^2 \qquad (4)$$

where KE is the impact energy, m is the droplet mass and V is the impact velocity. Plotting the kinetic energy given by this equation for a range of droplet diameter across the potential range of impact velocities, gives the values shown in figure 16.
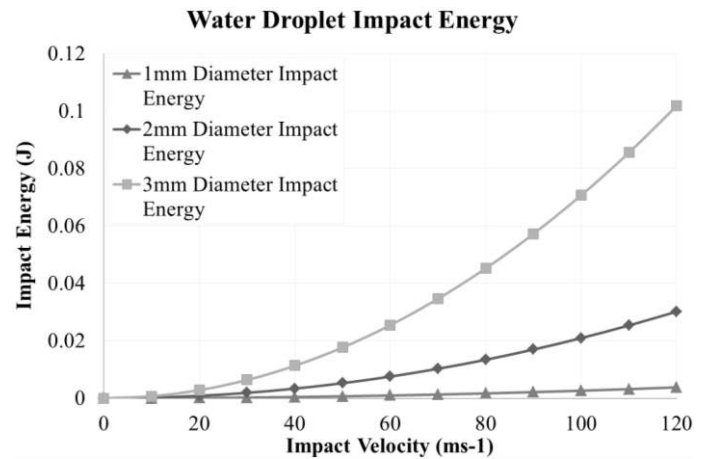

Figure 16. Water Droplet impact energy for a range of droplet diameters at various impact velocities, assuming a water density of 1000kgm^{-3}.

As shown, the droplet diameter plays a significant role in the impact energy associated to a given rain drop. The squaring effect of the impact velocity also has a strong influence on the impact energy. The energies shown may not be deemed significant in many engineering disciplines, however, given the significant duration of the exposure of the blades to these conditions and factoring in the other hostile environmental conditions, the energies take on greater significance.

Gohardani [28] states that in aviation studies a parameter often utilised for evaluating the erosion performance of materials under liquid impingement is the damage threshold velocity (DTV). This value is simply the lowest impact velocity at which damage in the target material is observed. The exact classification of such damage is not established, with some defining it as a loss of optical transmission or mass and others basing it on the occurrence of fracture [28]. Evans et al. [50] defined a theoretical expression for the DTV given by

$$V_{DT} \approx c_w 1.41 \left(\frac{K_{IC}^2 c_R}{\rho_w^2 c_w^2 d_w} \right)^{1/3} \qquad (5)$$

whereby, V_{DT} is the DTV, K_{IC}^2 is the fracture toughness of the target material, c_R is the Rayleigh wave velocity of the target material, ρ_w and c_w are the density of the water and compressional wave speed in the water respectively and d_w is the droplet diameter. Gohardani [28] describes that the Rayleigh wave is created (and confined) on the target surface and is responsible for ~2/3 of the impact energy. The Rayleigh wave velocity in a solid is given by [51]

$$c_R = \left(\frac{0.862 + 1.14\nu}{1 + \nu}\right)\left(\frac{E}{2(1+\nu)\rho}\right)^{1/2} \quad (6)$$

where c_R is the Rayleigh wave velocity, ν is the Poisson's ratio of the material and E is the Young's modulus.

Using both equations 5 & 6, it is possible to evaluate an approximate DTV for a typical wind turbine blade epoxy based coating. The material properties of typical epoxy gel coat technologies vary vastly between products and manufacturers, however assuming a typical Young's modulus of 3.2GPa, a Poisson's ratio of 0.38 and a density of 1150kgm^{-3}, equation 6 gives a Rayleigh wave speed of approximately 942ms^{-1}. This value can then be substituted into equation 5 to derive the theoretical approximate for the DTV for a range of rain droplet diameters; assuming a water density of 100kgm^{-3} and a compressional wave speed in water of 1490ms^{-1}. However, the fracture toughness properties of epoxy material systems can vary widely from low values of 0.5 to higher values of 1.5MPa.m$^{1/2}$ [52]. Therefore, the values of DTV across a range of rain drop diameters can be calculated using 3 different fracture toughness values of 0.5, 1 & 1.5 MPa.m$^{1/2}$. The DTV values obtained across a range of potential rain drop diameters (and for the three toughness values) are shown in figure 17.
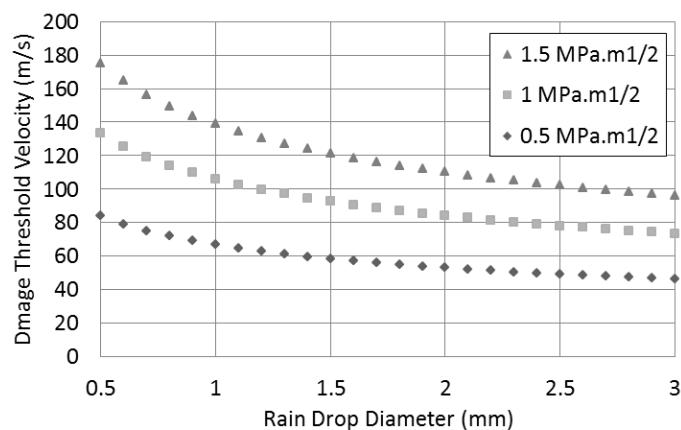

Figure 17. Damage Threshold Velocity for rain drop impact on an epoxy target across a range of droplet diameters and for different epoxy fracture toughness values

This plot highlights the importance of employing a surface coating technology with heightened fracture toughness. For low values of fracture toughness, the DTV value could potentially be as low as 50ms^{-1} for larger droplet sizes. However, it is also to possible to observe that even for tougher values, the DTV value can still be lower than 100ms^{-1} for large droplet sizes. This approach assumes normal impact angles and therefore represents the worst case scenario for liquid droplet impact, but it is prudent to note that the ranges of DTV values are not far removed or significantly higher than some of the tip speed values discussed previously. Additionally, the DTV value predicts the minimum required impact energy to induce instantaneous damage; therefore impact velocities slightly below the DTV values may still induce damage over a longer period or after repeated impact.

There exist many more propose analytical methods for predicting liquid droplet impact induced erosion and the methods discussed represent only a small insight into a vast area of research. However, many of the analytical approach devised and designed are targeted at the erosion behaviour of particular material classes or for certain impact conditions, and therefore care must be taken to fully understand the nature of the models before implementing them any other context. Furthermore, as highlighted by Gohardani [28] (in reference to aviation studies), the introduction of composite and advance polymer material technologies (as is also the case with wind turbine blades) presents added complexity to the approach of analytically predicting liquid impingement erosion.

7.4 Rain drop impact modelling

The benefits, challenges and limitations of analytical approaches to predicting and understanding rain erosion have been discussed. One approach to further understanding both the nature and significance of rain droplet impact on the leading edge is to conduct numerical modelling of the phenomena.

The capability to numerically model the phenomena of liquid impact on solid surfaces has historically been hindered by a lack of both available computational power and software techniques. However, advancement in both the power and affordability of computational resources in the past two decades has seen increased efforts to effectively model liquid-solid impact interactions. Adler [53] conducted some of the earliest finite element analysis studies, investigation the impact of water droplets on a solid polymeric target. The approach utilised a wholly Lagrangian meshing method for both the target and the water droplet. The modelling work was

found to completely encapsulate the temporal and spatial aspects of a liquid droplet impacting a solid surface, capturing the spreading phenomena. The study also has the relative advantage of being able to model the target material response during impact and therefore evaluate the stresses and strains during impact. Further potential to include damage propagation effects are also discussed.

Keegan et al. [54] also conducted numerical modelling of rain droplet impact on typical wind turbine blade composite polymers. However the approach implemented in the study utilised a combined Eulerian-Lagrangian approach in ANSYS Explicit Dynamics software [55]. The study looked to evaluate the accuracy of using an Eulerian modelling approach to model water droplet normal impact on solid surfaces. The water droplet material was modelled using a Gruneisen equation of state and the target body consisted of an epoxy resin plate. The waterhammer equation (equation 1), modified waterhammer equation (equation 2) and the instantaneous impact force equation (equation 3) were used as a means of numerical-analytical validation. The validation of the modelling approach was not only concerned with the magnitude of the forces and pressures/stresses created, but also the spatial and temporal aspects of droplet-surface impact events. The study found that the approach was successful in meeting both these criteria, firstly in capturing the spatial development of rain droplet impact, as shown in figure 18, which shows the characteristic spreading droplet behaviour as characterised in many other studies [53] [45].
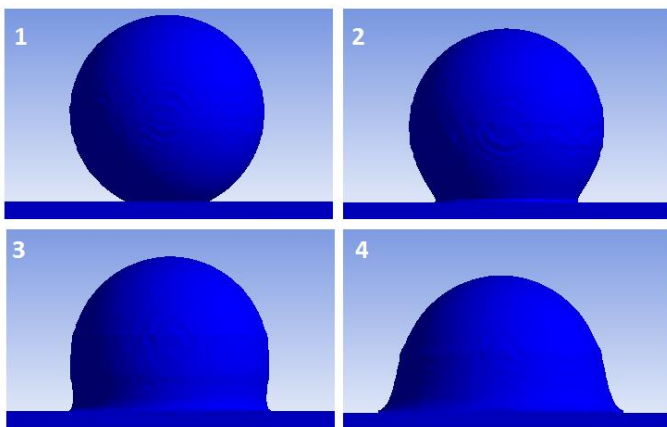
Figure 18. Impact development of a 3mm diameter raindrop impacting a solid surface at 140ms^{-1}. Source: **[54]**

Secondly, the study quantified the range of possible stresses created in a typical epoxy resin – an approximate representation of a gelcoat – for a 3mm diameter raindrop

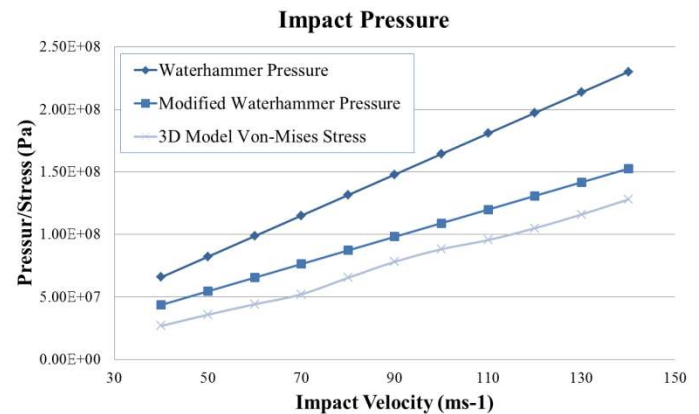impact, across a range of velocities, as shown in figure 19.

Figure 19. Von-Mises Stress created in an epoxy resin target during a 3mm diameter rain drop impact, modelled through a combined Eulerian-Lagrangian approach. The analytically obtained values for the waterhammer pressure (equation 1) and the modified waterhammer pressure (equation 2) are also plotted for reference. Source: **[54]**

As shown, the potential stresses created through direct normal raindrop impact can be significant. Stresses in excess of 50MPa can be generated at impact speeds as little as 70ms^{-1}. In many polymer matrix and coating systems, this level of stress could be considered significant in terms of approaching or exceeding the yield stress of the material. For instance, wind turbine blade materials manufacturers such as Gurit [56] provide the material properties for many of their products, and from reviewing the material data, a tensile strength of around 70MPa (dependant on cure time) is stated for many of their epoxy resin matrix material systems [57] [58].

Furthermore, although the numerical approach conducted by Keegan et al. [54] did not look at multiple near sited droplet impacts, variations in impact angle, repeated impact or incorporate any pre-stress in the material (from blade bending), these, in addition, may further increase the potential stresses created during impact. The effects of surface defects – through either manufacturing or handling - can also act as a seeding point for further wear and erosion. Given these factors and the probability that any single location on a blade surface may be repeatedly subjected to numerous impact events of this nature during the turbine lifetime, it is evident that phenomena of rain droplet impact erosion on the leading edge may indeed pose challenges for the material integrity of the blade surface. However, further parametric analysis would be required to fully understand these factors, and the use of experimental validation would also strengthen the

confidence in the numerical approach and results provided.

7.5 Experimental rain erosion testing

Although recent advances in computational technology and the development of sophisticated finite element analysis software tool have made modelling rain droplet impact possible, classically, experimental evaluation of rain erosion was widely practised in aerospace studies. As well as giving context to the issues of leading edge erosion in aviation (discussed previously) Gohardani [28] also discusses, at length, the experimental approaches to evaluating the rain erosion performance of aerospace materials.

The Rain Erosion Test Facility at the University of Dayton Research Institute, USA [26], has played a central role in a wide range of different rain erosion studies in the field of aviation; as have many other similar facilities [59] [60] [61]. The facility utilises a swirling arm apparatus, whereby a material sample is attached to the end of a rotating arm (driven by a motor) and rotated through a simulated rain field, as shown in figure 20.
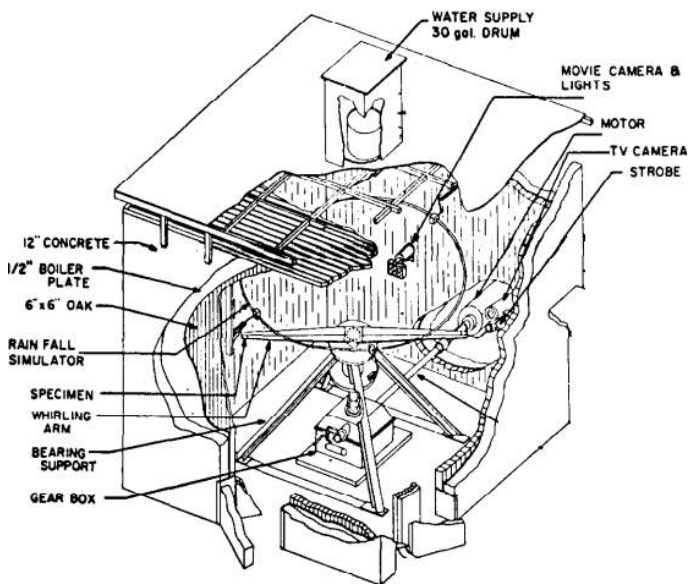

Figure 20. Rain Erosion Test Facility at the University of Dayton Research Institute **[26]**. Source: Image adapted from **[62]**

The facility can reach impact velocities of up to 650mph and can be run for prolonged durations, therefore allowing for the accelerated lifetime evaluation of the rain erosion resistance of the material sample tested. Rain erosion testing standards such as the 'ASTM G73-10 Standard Test Method for Liquid Impingement Erosion Using Rotating Apparatus' [63], provide guidance on the proper approach and methods for rain erosion testing and the appropriate and expected outcomes.

Polytech [24] offer rain erosion testing services, focussing primarily on the erosion of wind turbine blade leading edge materials and coatings. The company has performed testing for a long list of leading wind turbine material and coatings manufacturers. They too utilise a swirling arm apparatus configuration, working to the ASTM G73-10 standard as described.

8. Hailstone impact & erosion

8.1 Exposure

Wind turbine blade exposure to hailstone impact is a very site specific issue (more so than rain). As with the rain fall maps shown previously (figure 9) it is also possible to use climatic maps to examine the likelihood of hailstorm events across the UK, through the use of the map shown in figure 21.
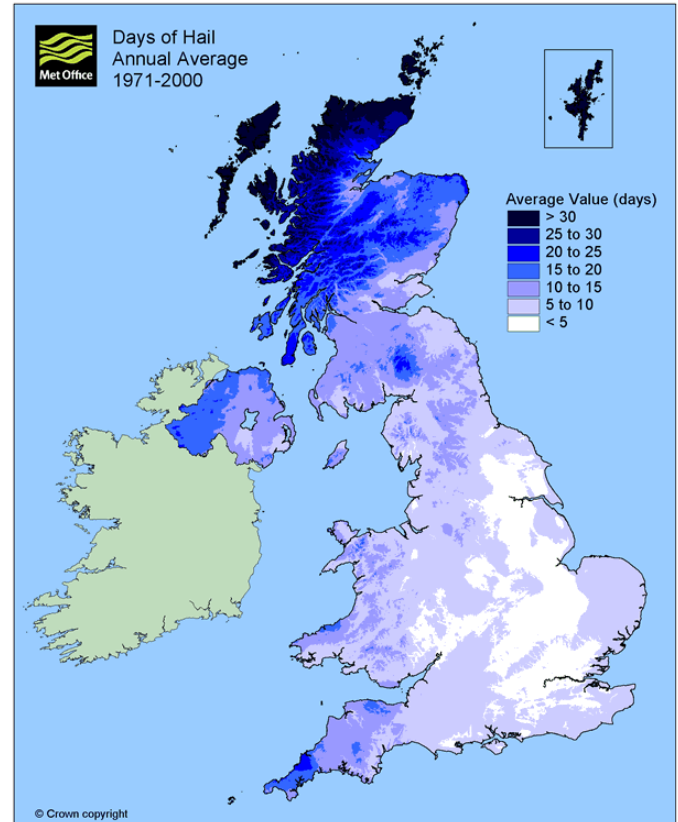

Figure 21. Days of hail, annual average from 1971-2000. Source: **[37]**

15

The map plots the annual average total days with hail in the UK using data covering the period of 1971-2000. From the map, it is clear that even within the relatively small geographical area of UK, there is a wide variability in the frequency of days with hail. In south eastern and central regions of England and around the Greater London area, the occurrence of hailstorms is somewhat rare i.e. less than 10 days over a year. It could therefore be said that in these regions, the threat posed by hailstone impact damage to the blade leading edge may be minimal. However, there still may be possibilities of freak hailstorm events, as the maps say nothing of the magnitude or the intensity of the hailstorm event. It is clear though that in more north eastern regions, specifically in Scotland, that the frequency of hailstorm events is much higher, with some areas in the Highlands and Western Isles experiencing more than 30 days with hail in a year. In these regions, it may indeed be critical to consider the effects of hail impact and erosion on the blade leading edge. Outside the UK, the same degree of variability in the frequency of hailstorm events can also be observed. For example, reviewing data from the Irish Meteorological Service [64] it can be seen that in some locations such as Malin Head in the North of Ireland there may be up to 48 days with hail events in a year (averaged over 30 years), whereas in other sites such as Roches Point, in the South of the country, Cork, the total average only comes to 8 days with hail in a year. Again, this highlights the necessity for a thorough understanding of the typical meteorological conditions for any proposed (or operational) site.

8.2 Hailstone impact characterization

Convention states that a hailstone has a diameter of at least 5mm, whereas smaller particles are referred to as ice pellets or snow pellets. Hailstones are formed in cumulonimbus clouds (thunder clouds), especially those with a strong updraft, large liquid content, large vertical height and large cloud-drop sizes [65]. In these thunderclouds, drops of water rise up through the cloud and begin to freeze, once reaching a certain mass the ice particle will descend through the cloud. Some of these ice particles are then again caught in the updraft and acquire an additional layer of ice and this process of updraft and downfall can recur several times for any given particle. Through each cycle the particle will acquire an additional layer of ice until the thundercloud can no longer support

its weight and it falls to earth as hail. It is this cyclic layering process that gives hail its onion like formation, as shown by the cross section of a large hailstone in figure 22.

Figure 22. Cross section of a large hailstone, showing the onion-like layered formation. Source: **[66]**

The average size of hailstones is dependent on site location and established average values are difficult to accurately ascertain. The only certain way to establish the likely average size of hail at any given site would be through measurement on location. In the UK, some of the largest ever recorded hailstone sizes are in the range of 60-90mm [67], however these are considered freak events.

The consequences of these large diameters in the context of impact considerations (specifically in comparison to rain drop impact) play an important factor in two ways. Firstly, with an increase in diameter there is also an increase in the hailstones mass and therefore an increase in its impact energy, as described previously by equation 4. Additionally, with increased diameter and subsequent mass, the terminal velocity also increases according to the relationship shown in equation 7, where V_t is the terminal velocity, g is the gravitational acceleration, C is the drag coefficient (0.5 for a sphere), ρ_{air} is the air density and A_h is the cross sectional area of the hail stone in the direction of travel [68].

$$V_t = \sqrt{\frac{2m_h g}{C \rho_{air} A_h}} \qquad (7)$$

This equation is derived from balancing the gravitational forces pulling on the falling body with the aerodynamic drag forces acting to slow the fall. Although not applicable to all hailstone impact events, it acts as a useful guide to the range of possible terminal velocities. Using this equation, assuming a density of 900kgm^-3 for the hailstone (this value varies widely, as will be discussed) and 1.29kgm^-3 for air, and assuming a

perfectly spherical hailstone shape and thus a drag coefficient of 0.5, it is possible to plot the theoretical terminal velocity for a range of hailstone diameters, as shown in figure 22.
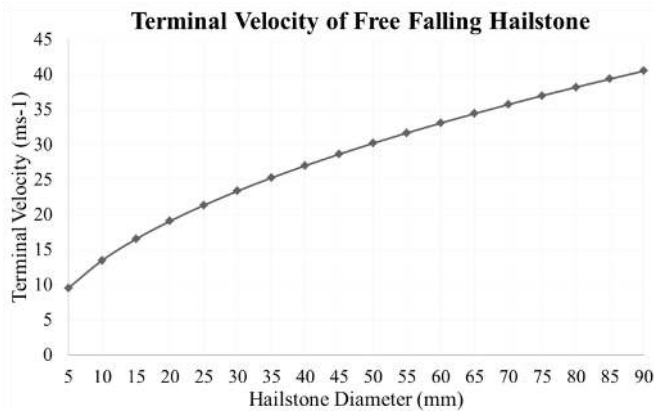

Figure 23. Terminal velocity of free falling hailstone of varying diameter, according to equation 7. Assuming: Ice density of 900kgm^{-3}, air density of 1.29kgm^{-3} and a drag coefficient of 0.5.

Figure 23 shows the effects of the increased diameter and mass of the hailstones – in comparison to rain – on their theoretical terminal velocity. Adopting the same vector analysis as previously implemented to evaluate the impact velocity of rain drops on a wind turbine blade (figure 13); it is also possible to evaluate the possible maximum hailstone-blade impact velocity. Figure 24 shows the maximum calculated impact velocity of both a 15mm and 30mm diameter hailstone, impacting a blade tip with a tip speed of 90ms^{-1}, in a 20ms^{-1} wind field. The previous results obtained for rain drops in these conditions are also shown for comparison; as is the constant tip speed for reference.
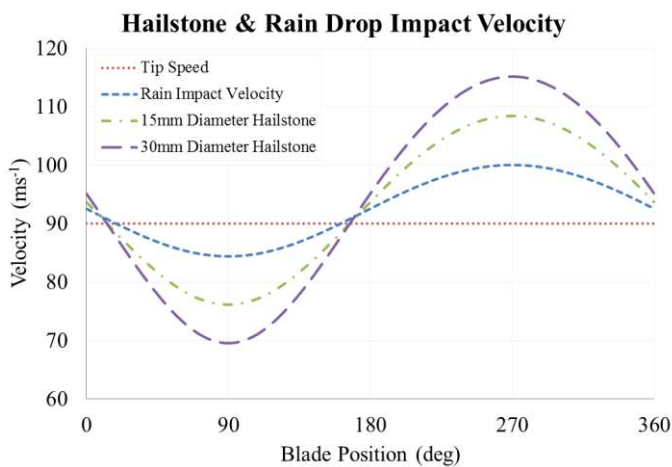

Figure 24. Hailstone impact velocity for a 15mm and 30mm diameter hailstone, fully entrained in a 20ms^{-1} horizontal wind, striking a blade tip with a 90ms^{-1} tip speed. The tip speed has also been plotted for

reference, as has the impact velocity for the rain drop shown previously in figure 13.

It is clear from figure 24 that as expected, the increased terminal velocity of hailstones (compared to rain drop) results in higher maximum impact velocities during the upswing phase of blade rotation (180-360˚); and a reduction in the minimum impact speed.

As stated, the density of hail ice can vary widely between locations and storms. Field et al. [69] state that for hail sizes smaller than 20mm in diameter, densities can range widely from 50 to 890kgm^{-3}, but for larger sizes higher densities in the range of 810 to 915kgm^{-3} are observed. For the purposes of hail threat standardisation (for aerospace applications), they establish that it is reasonable to assume a worst case density of 917kgm^{-3} (solid ice) for hailstones.

As with rain impact, it is again useful to quantify the potential ranges of impact energies associated with hailstone impact. Take for example a hailstone ice density of 850kgm^{-3}, it is possible to calculate (using equation 4) the impact energy for a range of diameters, across a range of potential impact velocities, as shown in figure 25. From this, it is apparent just how important the diameter (and therefore the mass) of the hailstone is in determining the potential impact energy that it may impart during impact.
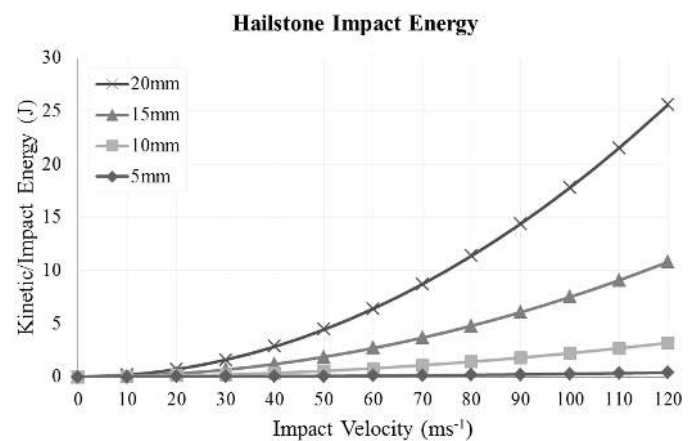

Figure 25. Hailstone impact energy for a set of hailstone diameters (5, 10, 15, 20mm) across a range of impact velocities, determined using equation 4.

It also clear, through comparison with the impact energy values for rain drop impact shown in figure 16, that the potential ferocity of hail impact is far greater than that of rain impact.

8.3 Hailstone impact modelling

As with rain impact, numerical modelling can play an important role in understanding both the nature of hailstone impact and the response of the material technologies used in the blade leading edge. However, in order to perform such modelling approaches, the material behaviour of ice needs to be well understood and characterised. This is not a trivial exercise however, as the variability in size and density are not the only challenges in establishing characteristic hailstone properties for the consideration of impact on the leading edge of wind turbine blades. The material properties of hailstones are also inherently variable. Schulson [70] states that ice may exhibit two types of inelastic behaviour when loaded under compression. When loaded at low strain rates ice behaves in a ductile manner; however with increasing strain rate it begins to behave in a more brittle manner, as indicated by figure 26.
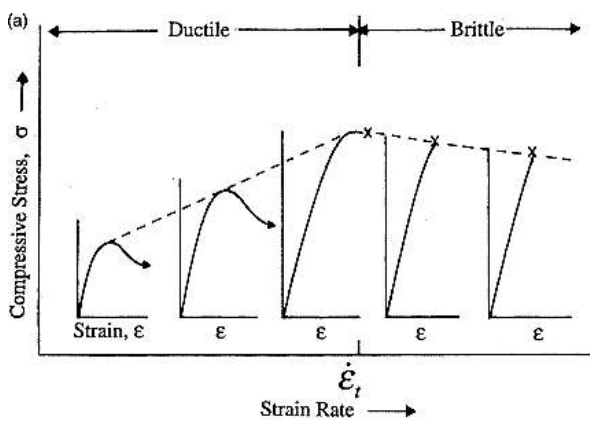

Figure 26. Schematic diagram showing the ductile to brittle transition in the behaviour of ice under increasing strain rates, whereby ε_t marks the theoretical point of transition. Source: **[70]**

Carney et al. [71] summarized that polycrystalline and single crystal ice exhibit strain rate sensitivity from $10^{-8}s^{-1}$ to $10^{-2}s^{-1}$ and that single crystal ice has also been shown to be rate sensitive in the range of $\sim 10^0$ to 10^3. This strain sensitivity of single crystal ice at high strain rates was established through plotting data from tests conducted by Shazly et al. [72] and fitting it to a trend using a static strength of 14.8MPa, as shown in figure 27 [71].
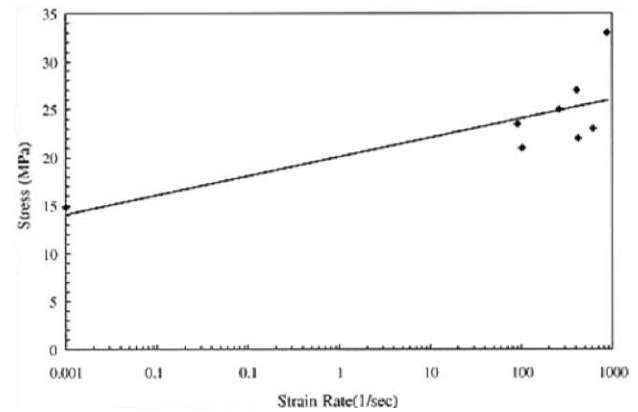

Figure 27. Strain rate sensitivity of single crystal ice under compression. Source: **[71]**

The variability of the material properties of ice highlight the challenges in confidently predicting the forces and stress imparted on the blade from a potential hailstone strike. However, regarding quantifying the magnitude of impact forces and stresses, it should be acceptable to establish an approximation to the likely properties of hailstone ice, as classifying a standard hailstone impact is approached with some difficulty.

As with rain drop impact, several approaches to numerically modelling hailstone impact have been proposed in previous studies [71] [73] [74] [75] [76]. The most developed and established approach was proposed by Carney et al. [71], who developed a material model for ice for the purposes of evaluating the threat of ice impact on aerospace components. The model was developed for use in LS-DYNA software [77], using an Eulerian approach to model the ice projectile. The material model developed employs a method of modelling the strain rate sensitive nature of ice, meaning that unlike previously proposed ice material models, no parametric tuning is required for different impact conditions. The accuracy of the numerical model was validated through experimental work to give full confidence in the results obtained numerically. Keegan et al. [78] considered the ice material model developed by Carney et al. [71] to investigate the effects of hailstone impact on the leading edge of a wind turbine blade. The work utilised a Smooth Particle Hydrodynamics (SPH) approach instead of an Eulerian approach to model the ice, in light of the comparative accuracy but much reduced computational requirements; as summarised by Anghileri et al. [79]. Keegan et al. [78] first validated the compatibility of SPH approach with the material model

18

defined by Carney et al. [71] and subsequently implemented the material model to study hailstone impact on a typical wind turbine blade leading edge profile. The leading edge profile geometry and material properties were ascertained from industrial consultation and were established as being representative of a typical utility scale blade tip. The leading edge profile featured a 3 ply biaxial glass-fiber/epoxy composite laminate [+45/0/-45], with a glass/epoxy chopped strand mat composite (CSM) protective layer and a surface coating of epoxy gel coat. The study used the ice material model to simulate direct normal impact on the curved leading edge of the profile, varying both the hailstone diameter between 5, 10 & 15mm and the impact velocity from 70-120ms^{-1}. Figure 28 shows the development of a 10mm diameter hailstone impacting the leading edge profile at 100ms^{-1}, plotting contours of von-Mises stress for each time step taken. The plot shows the inner and outer surfaces during impact and highlights that when considering hailstone impact, the regions of significant stress and strain creation are not isolated to the coating systems and the effects of impact are borne throughout the blade skin thickness.

A summary the maximum stresses created in the leading edge profile during impact for the range of conditions simulated by Keegan et al. [78] are shown in figure 29.
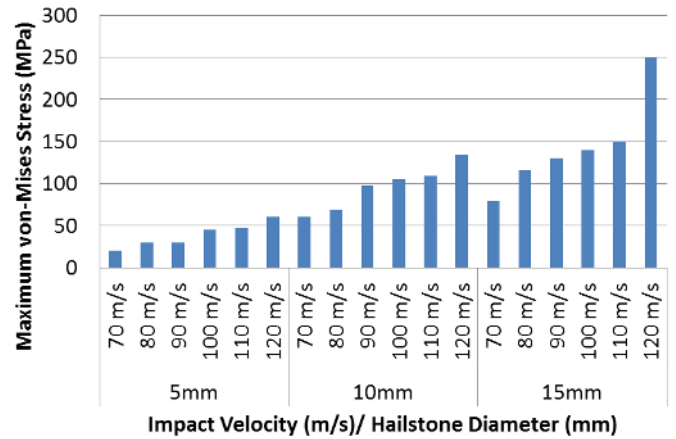
Figure 289. Maximum von-Mises stress created in the blade leading edge materials during simulated hailstone impacts of varying diameter and velocity. Source: **[78]**

As shown, the magnitude of the stresses created in the materials during impact from hailstones of 10mm diameter and greater, far exceed those generated during rain drop impact [54]; as shown in figure 19. This increase in ferocity comes from the increased mass of the hailstones and the subsequent heightened impact energy. In the study, the capability of LS-DYNA to predict material erosion - through specifying a failure strain for the material - brought on through hailstone impact [78]is also utilised. Figure 29 shows the modelled erosion on the leading edge of the profile resulting from a 15mm diameter hailstone impact at 100ms^{-1}. It shows the removal of part of both the epoxy gelcoat layer (blue) and
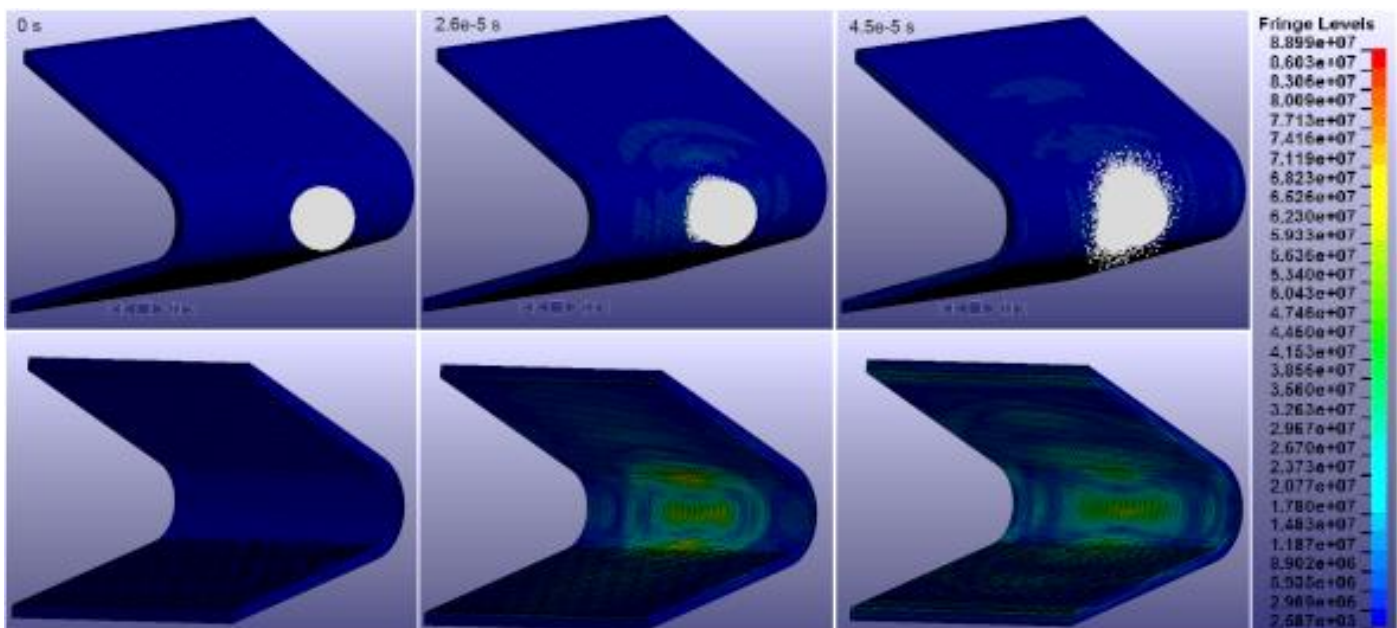
Figure 28. Development of a 10mm diameter hailstone impacting a blade tip leading edge at 100ms^{-1}, showing contours of von-Mises Stress on the outer (upper images) and inner (lower images) surfaces. Source: [65]

the chopped strand mat composite layer (green), resulting in the exposure of the composite laminate below (yellow). Although the results are based on approximate estimates of the failure strain of the materials involved (in the absence of available data), the approach does present a method that (with experimental validation) could prove a powerful design and evaluation tool for blade development.
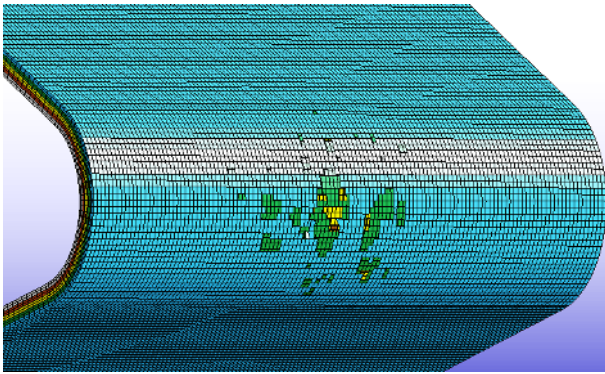

Figure 29. Modelled leading edge erosion from a 15mm diameter hailstone impact at 100ms^{-1}. Source: **[78]**

It is important then to address the effect increased impact energies may have on the material performance of the leading edge. As with rain impact, the repeated – or in the case perhaps of extreme hailstone sizes, singular – impact of hailstones may lead to erosion of the leading edge. The influence of surface defects may again play and important role in the development of such erosion. The consequences of leading edge erosion are identical to those previously discussed in relation to rain erosion above. It is important, however, to understand all the potential modes of damage brought about through hail impact, as discussed in the following section.

8.4 Hailstone impact damage modes

As identified by Keegan et al. [78], hailstone impact can result in stress propagation throughout the blade skin thickness. Therefore, surface erosion is not the only possible material failure mode, as failure in the substrate could also be an issue for impact events with sufficient energy. Through a combination of both shear and normal stress transfer between composite plies, delamination between plies may occur. The effects of delamination can be significantly detrimental to the static and fatigue properties of the laminate and may also result in further propagation of the delamination between plies. The constituents of the composite material may also fail independently (or together) resulting in cracking through

the matrix material or crushing of the reinforcing fiber. Both can have a significant effect on static and fatigue properties of the material.

Prayogo et al. [80] investigated the fatigue damage effects of repeated raindrop collisions on chopped strand mat glass fiber reinforced epoxy composite laminates. Using 4mm diameter nylon beads to represent raindrops, the samples were subjected to repeated impact and systematically inspected for signs of damage. Through this approach it was possible to establish the number of impact events required for the onset of material damage in the composite laminates, as shown in figure 31.
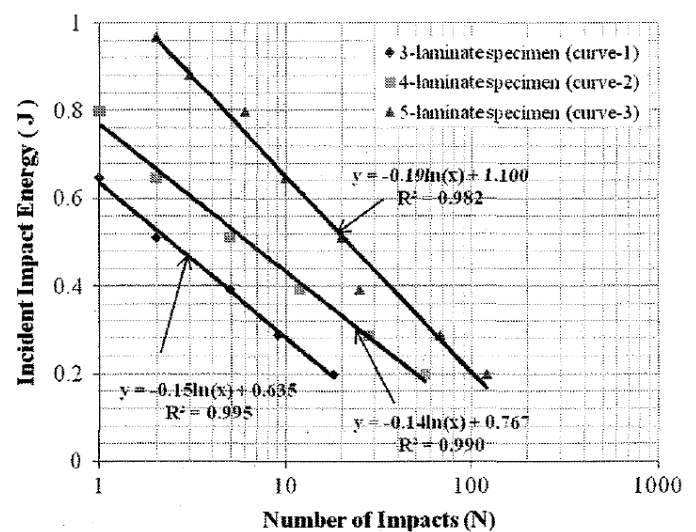

Figure 30. Impact fatigue damage in chopped strand mat glass fiber/epoxy composite laminates of varying ply numbers. Showing the number of impact events at specified impact energies required for the onset of material damage. Source: **[80]**

The work states that for each sample, internal damage was the first to take place in the form of interface debonding between the polymer matrix and reinforcing fiber. The damage then progressed to the surfaces in the form of star cracking on the rear of the samples and ring cracking on the front face of the samples, leading eventually to delamination of the plies. Debonding between the fiber and matrix is attributed to tensile stress waves during impact and microvoid nucleation, growth and coalescence is attributed to delamination; in which shear stress is deemed to play a significant role [80]. It is prudent to note that the impact energies considered in figure 31 are well within the range of the hailstone impact energies detailed in figure 25 and although the samples considered by Prayogo et al. [80] were unprotected bare laminates of CSM - which are typically

weaker than that of unidirectional or weaved reinforced composites - it highlights the threat posed by such impact energies.

The damage mechanisms described are not mutually exclusive and are only a few of the possible types of damage. It may be the case that a combination of many failure mechanisms may manifest as a result of either single or repetitive hailstone impact. Damage induced through impact has been shown to reduce both the static compressive [81] and tensile [82] strength of composite materials. However, impact damage may not only affect the static structural properties of the composite substrate, but may also greatly degrade the load bearing fatigue properties of the material. Many studies have shown that transverse impact can markedly reduce the fatigue life properties of glass fiber reinforced composite materials in a load bearing capacity [82] [83]. Yuanjian & Isaac [82] studied the tension-tension fatigue behaviour of glass fiber reinforced polyester composite laminates after being subjected to low velocity transverse impact at varying levels of energy. The study found that the ply orientations of the laminate strongly influenced the post impact tensile properties. For example, the tensile and fatigue properties of a [±45˚]$_4$ laminate were seriously impaired at relatively low impact energy levels, whereas for a [0/90˚]$_{2s}$ laminate, the tensile properties (and consequently the fatigue life) only began to degrade above a critical impact energy. Figure 31 shows the post-impact fatigue life of the [±45˚]$_4$ laminate samples, for varying levels of impact energy. It shows that for impact energies of 1.4J, very little effect on the fatigue properties are observed (compared to 0J). However at higher impact energies the effects on the fatigue performance are substantial.
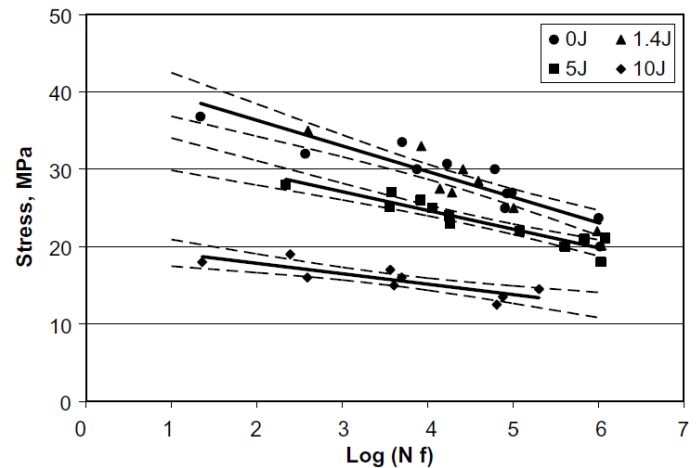

Figure 31. S-N fatigue data for a glass fiber reinforced polyester laminate of [±45˚]$_4$ configuration, following impact at 0, 1.4, 5 & 10J. Source: [69]

Again, it is important to note that the impact energies considered by Yuanjian & Isaac [82] are not out-with the proposed range of potential impact energies imparted by hailstone impact, as shown in figure 25. Such reductions in the fatigue strength of wind turbine blade composites would prove very damaging to the material and lifetime performance of the blade; made worse by the very fact that blades undergo almost constant cyclic loading.

8.5 Experimental hailstone impact evaluation

Experimental analysis of ice impact is an area of research in which (most commonly alongside numerical evaluation) a considerable amount of previous work has been conduct. Most commonly, singular impact events are simulated through use of cannon apparatus, power by compressed gas reservoirs. Carney et al. [71] adopted such an approach when conducting experimental work for the purpose of validating the ice material model developed; although the work looked at the impact of ice cylinders rather than hailstone like geometries. Similarly Kim & Kedward [73] also utilised an ice cannon when conducting hailstone impact research, the results of which were also used to validate a proposed numerical ice material model. Through use of strain gauges, force measurement transducers and other apparatus, it is possible to closely record both the impact forces and strains during a given impact, thus helping to develop a greater understanding of the impact and, if applicable, validating any numerical approaches adopted. There is no established method by which to conduct high frequency repetitive hailstone impact exposure testing (like that of rain erosion testing), however it may be that a rotating

rain erosion test setup could be adapted to test for repetitive hailstone impact.

9. Sea spray

For offshore wind turbines the issue of impact on the blade from spray whipped up from the sea surface may also present a threat to the leading edge of the blades. The nature of sea spray impact on the blade will most likely be very similar to that of rain with respect to the forces and pressures exerted and the development of individual impact events. However in some situations, larger volumes of sea spray water may impact the blade instantaneously. Another consideration with regards to particulate impact on the blade, when considering sea spray, relates to the transport of sea salt crystals in the sea spray. Airborne sea salt crystals can be an issue in many offshore applications, leading primarily to accumulation on components, which is cited as an issue from many sources [84] [85] [86]. In addition, with sea water containing 3-3.5% NaCl typically [87], corrosion may be a significant issue for any metallic constituents. Therefore, salt crystals – through accumulation on the blade leading edge – may lead to degradation in the aerodynamic performance of the blade; rather than any erosive effect and possibly lead to corrosive damage also. However, to date, there has been little research on this topic.

10. Sand, dust and other particulate matter

As with all other causes of leading edge erosion, exposure to sand, dust and other extraneous matter is often cited as a problem (as referenced to in section 4). As with all forms of environmental exposure, these will be heavily site dependant. In warm and arid climates, sand and dust may be a common type of airborne particulate and therefore may pose leading edge erosion problems, whereas in wetter, greener habitats the problem may be non-existent. Likewise, at near shore locations, the issue of sand erosion may be a considerable threat.

Finite element modelling techniques can be employed to better understand the nature and potential effects of sand and dust impingement on a blade leading edge. Numerous studies have looked at modelling solid particulate impact and erosion on solid target bodies

across a variety of research fields and using both commercial and purpose made models [88] [89] [90] [91] [92]. As with rain and hail modelling, these approaches could be utilised as both a design and evaluation tool for the blade leading edge.

Experimental approaches to evaluating the effect of sand erosion can also be adopted through use of simple sand blasting techniques. However as with rain erosion testing, this approach will only act to inform on the potential resulting damage modes and the erosive resistance of certain materials, but will reveal little about individual impact development; this may be explained by the numerical approaches discussed.

14. Conclusions

The area of wind turbine blade leading edge erosion is still a developing area of research and as such the frequency and severity of the problem is still uncertain. Furthermore, the effects of increasingly large blades, and consequently high tip speed values, on the issue of leading edge erosion is not yet fully understood. As currently operational technologies mature, it is likely that there will be many lessons learned and a greater understanding developed.

However, as discussed above, there are various tools and techniques available to developers, manufacturers and operators which may be used as a guide in evaluating and potentially mitigating the risk posed by leading edge erosion:

1. Climatic maps and meteorological data, (together with erosion maps if available), can be utilised to assess the probable environmental conditions in which a given sited turbine may operate in, therefore enabling assessment of the threat posed by different types of environmental variable.
2. Experimental rain and hailstone exposure testing can also provide useful information regarding the performance of certain leading edge material technologies under certain impact conditions.
3. Numerical modelling approaches can be used in the blade design process to better understand the material response of the blade following impact from airborne particulates and the likelihood of erosion.

Using these tools, coupled with operational field data (if and when it becomes available), may help to broaden and develop a greater understanding of the potential causes and factors contributing to blade leading edge erosion. However, it is clear from the review conducted, that the many environmental factors and the ever growing scale of modern wind turbine blades, present significant challenges in both mitigating against leading edge erosion issues and design of higher performance materials for exposure to such environments.

Acknowledgements

References

[1] Wilkes J, Moccia J 2013 Wind in power: 2012 European statistics *EWEA Annual Report*

[2] The European Wind Energy Assoiation, 2012. [Online]. Available: www.ewea.org. [Accessed February 2013].

[3] Paska J, Salek M and Surma T 2009 Current status and perspectives of renewable energy sources in Poland *Renewable and Sustainable Energy Reviews* **13** 142-54,.

[4] Quarton D 2013 Wind energy technology and the research challenge *Wind Energy Centre for Doctoral Training Inaugural Seminar: FutureWind (Glasgow, UK, 16, January 2013)*

[5] Mishnaevsky J L, Brøndsted P, Mijssen R, Lekou D J and Philippidis T P 2011 Materials of large wind turbine blades: recent results in testing and modelling *Wind Energy* **15** 83-97

[6] Jackson K J, Zuteck M D, van Dam C P, Standish K J and Berry D 2004 Innovative design approaches for large wind turbine blades *Wind Energy* **8** 141-71

[7] Buckney N, Green S, Pirrera A and Weaver P M 2012 On the structural topology of wind turbine blades *Wind Energy*, **Early View**

[8] 3M 2012. [Online]. Available: http://multimedia.3m.com/mws/mediawebserver?mwsId=66666UF6EVsSyXTtoXT6l8T2EVtQEVs6EVs6EVs6E666666--&fn=WindErosionControlBrochure_DMR_9. [Accessed March 2013].

[9] LM Wind Power 2013 Reliability guarantees maximum output [Online] Available: http://www.lmwindpower.com/Rotor-Blades/Technology/Design/Reliability. [Accessed

[10] Gurit, 2013 Coatings [Online]. Available: http://www.gurit.com/coatings-1.aspx. [Accessed April 2013].

[11] Haag M D 2013 Advances in leading edge protection of wind turbine blades *EWEA (Vienna, Austria, 4-7, February 2013)*

[12] 3M 2011 Wind Energy[Online] Available: http://solutions.3m.com/wps/portal/3M/en_US/Wind/Energy [Accessed April 2013]

[13] Wood K 2011 Blade repair: Closing the maintenance gap *Composites Technology* **April**

[14] Rempel L 2012 Rotor blade leading edge erosion - real life experiences *Wind Systems Magazine* **October**

[15] TGM Services 2011 Blade erosion [Online]. Available: http://tgmwind.com/bladeerosion.html#bladeerosion [Accessed April 2013]

[16] Henkel 2013 Blade maintenance [Online]. Available: http://www.henkelna.com/industrial/blade-maintenance-19836.htm. [Accessed March 2013].

[17] Broadwind Energy 2012 Blade services [Online]. Available: http://www.bwen.com/WindTurbineBladeServices_7777.aspx. [Accessed March 2012].

[18] Ropeworks 2011 Blade repair and maintenance services [Online]. Available: http://www.ropeworks.com/service_wind_blade.htm. [Accessed April 2013]

[19] Dalili N, Edrisy A and Carriveau R 2009 A review of surface engineering issues critical to wind turbine performance *Renewable and Sustainable Energy Reviews* **13**, 428-38

[20] v. Rijswijk K and Harald B 2006 Thermoplastic Composite Wind Turbine *Dutch Wind Workshops (Delft, Amsterdam, 11-12, October 2006)*

[21] Karmouch K and Ross G G 2010 Superhydrophobic wind turbine blade surfaces obtained by a simple deposition of silica nanoparticles embedded in epoxy *Applied Surface Engineering* **257** 665-69

[22] Sayer F, Bürkner F, Buchholz B, Stobel M, van Wingerde A M, Busmann H G and Seifert H 2013 Influence of a wind turbine service life on the mechanical properties of the material and the blade *Wind Energy* **16** 163-74

[23] Wind Turbine Models 2013 DFVLR DERBA-25 [Online]. Available: http://en.wind-turbine-models.com/turbine/429/dfvlr/debra-25. [Accessed 2013].

[24] Polytech Rain Erosion [Online]. Available: www.erosion.com [Accessed April 2013]

[25] Powell S 2011 3M wind blade protection coating W4600 *Industrial Marketing Presentation*

[26] University of Dayton Research Institute 2013 Rain erosion test facility [Online]. Available: http://www.udri.udayton.edu/NONSTRUCTURALMATERIALS/COATINGS/Pages/RainErosionTestFacil

ity.aspx [Accessed April 2013]

[27] Weigel W D 1996 Advanced rotor blade erosion protection system *Kaman Aerospace Corporation, Bloomfield*

[28] Gohardani O 2011 Impact of erosion testing aspects on current and future flight conditions *Progress in Aerospace Sciences* **47** 280-303

[29] Huang C W, Yang K, Liu Q, Zhang L, Bai J Y and Xu J Z 2011 A study on performance influences of airfoil aerodynamic parameters and evaluation indicators for the roughness sensitivity on wind turbine blade *Technological Sciences* **54** 2993-8

[30] Sareen A, Chinmay S A, Selig M S 2013 Effects of leading edge erosion on wind turbine blade performance *Wind Energ* Online

[31] Chinmay S A 2012 Turbine blade eorison and the use of wind protection tape *(Masters Thesis) University of Illinois*

[32] Calvert M E, Wong T –C, O Malley J A 2006 Blade contour deformation and helicopter performance *AIAA Applied Aerodynamics Conference (2006, San Francisco)*

[33] 3M 2011 A 3M study is the first to show the effects of erosion on wind turbine efficiency, [Online]. Available: http://www.pressebox.com/pressrelease/3m-deutschland-gmbh/A-3M-Study-Is-the-First-to-Show-the-Effects-of-Erosion-on-Wind-Turbine-Efficiency/boxid/445007. [Acessed April 2013]

[34] Shokreih M M and Bayat A 2007 Effects of ultraviolet radiation on mechanical properties of glass/polyester composites *Composite Materials* **41** 2443-55

[35] Kumar B G, Singh B G and Nakamura T 2002 Degradation of carbon fiber-reinforced epoxy composites by ultraviolet radiation and condensation *Composite Materials* **36** 2713-33

[36] Gurit 2013 Guid to composites [Online]. Available: http://www.gurit.com/files/documents/Gurit_Guide_to_Composites(1).pdf. [Accessed March 2013].

[37] Met Office 2013 Met Office - UK mapped climate averages [Online]. Available: http://www.metoffice.gov.uk/climate/uk/averages/ukmapavge.html. [Accessed March 2013].

[38] Climatic Research Unit 2013 Climatic Research Unit - University of East Anglia [Online] http://www.cru.uea.ac.uk/ [Accessed April 2013]

[39] ASTM 2013 ASTM G73 - 10 Standard Test Method for Liquid Impingement Erosion Usind Roatating Apparatus

[40] Elert G, Volynets I 2001 Diameter of a raindrop [Online]. Available: http://hypertextbook.com/facts/2001/IgorVolynets.shtml

[41] Villermaux E, and Bossa B 2009 Single-drop fragmentation determines size of distribution of raindrops *Nature Physics* **5** 697-02

[42] Kubilay A, Derome D, Blocken B and Carmeliet J 2013 CFD simulation and validation of wind driven rain on a building facade with an Eulerian multiphase model *Building and environment* **61** 69-81

[43] Best A C 1950 The size distribution of raindrops *Q J R Meteorological Soc* **76** 16-36

[44] R. Gunn and G. D. Kinzer, "The terminal velocity of fall for water droplets in stagnant air," Journal of Meteorology, vol. 6, pp. 243-248, 1949.

[45] Heymann F J 1969 High-speed impact between a liquid drop and a solid surface *Journal of Applied Physics* **40** 5113-22

[46] Dear J P and Field J E 1988 High-speed photography of surface geometry effects in liquid/solid impact *Journal of Applied Physics* **63** 1015-21

[47] Imeson A C, Vis R and de Water E 1981The measurement of water-drop impact forces with a piezo-electric transducer *CATENA* **8** 83-96

[48] Nearing M A, Bradford J M and Holtz R D 1986 Measurement of Force vs. Time Relations for Waterdrop Impact *Soil Science Society of America Journal* **50** 1532-6

[49] Du N and Elert G 2000 Speed of sound in water [Online]. Available: http://hypertextbook.com/facts/2000/NickyDu.shtml [Accessed April 2013].

[50] Evans A G, Gulden M E, Eggum G E, Rosenblatt M 1976 Impact damage in brittle materials in the plastic response regime *Rep No. SC5023 Rockwell International Science Center*

[51] Achenbach J D 1973 *Wave propagation in elastic solids* (North-Holland)

[52] Ashby M F, Shercliff H, Cebon D *Materials: Engineering, Science, Processing and Design* (Butterworth-Heinemann)

[53] Adler W F 1995 Waterdrop Impact Modelling *Wear* **186-187** 341-51

[54] Keegan M H, Nash D and Stack M 2012 Modelling rain drop impact of offshore wind turbine blades *ASME TURBO EXPO (Copenhagen, June, 2012)*

[55] ANSYS 2011 Explicit Dynamics Solutions [Online]. Available: http://www.ansys.com/Products/Simulation+Technology/Structural+Mechanics/Explicit+Dynamics [Accessed April 2013]

[56] Gurit 2013. [Online]. Available: www.gurit.com. [Accessed April 2013].

[57] Gurit 2013 Prime 27 [Online]. Available: http://www.gurit.com/files/documents/prime-27v4pdf.pdf. [Accessed April 2013].

[58] Gurit 2013 Prime 20LV [Online]. Available: http://www.gurit.com/files/documents/prime-20lvv10pdf.pdf. [Accessed April 2013].

[59] Diarkis 2013 San and Rain Erosion Testing [Online]. Available: http://diarkis.com/index.php/analytics/sandrain-erosion-testing [Accessed 2013]

[60] Saab 2013 Environmental Testing [Online]. Available:

http://www.saabgroup.com/Templates/Public/Pages/PrintAllTabs.aspx?pageId=34399 [Acccessed 2013]

[61] NAWCAD 2013 Rain Erosion/Impact Measurement Lab [Online] http://www.navair.navy.mil/nawcad/index.cfm?fuseaction=home.content_detail&key=A046A704-0218-4E12-882B-919322581DE0 [Accessed 2013]

[62] Zahavi J, Nadiv S 1981 Indirect damage in composite materials due to raindrop impact *Wear* **72** 305-13

[63] ASTM International 2011 Standard Test Methof for Liquid Impingement Erosion Using Rotating Apparatus *ASTM International, West Conshohocken*

[64] The Irish Meteorological Service 2013 30 year averages. [Online]. Available: http://www.met.ie/climate/30year-averages.asp. [Accessed April 2013].

[65] American Meteorological Society2012 Hail [Online]. Available: http://glossary.ametsoc.org/wiki/Hail.

[66] Wikimedia Commons, November 2009. [Online]. Available: http://commons.wikimedia.org/wiki/File:Hagelkorn_mit_Anlagerungsschichten.jpg.

[67] TORRO 2011 Hail Scale [Online] Available: http://www.torro.org.uk/site/hscale.php.

[68] Georgia State University 2012 Terminal Velocity [Online]. Available: http://hyperphysics.phy-astr.gsu.edu/hbase/airfri2.html

[69] Field P R, Hand W, Cappelluti G and A McMillan 2012 Hail Threat Standardisation *Met Office & QinetiqReport*

[70] Schulson E M 2001 Brittle failure of ice *Engineering Fracture Mechanics* **68** 1839-87

[71] Carney S K, Benson D J, DuBois P and Lee R 2006 A phenomenological high strain rate model with failure for ice *International Journal of Solids and Structures* **43** 7820-39

[72] Shazly M, Prakash V and Lerch B 2005 High strain rate compression testing of ice *NASA TM-2005-213966, 2005*

[73] Kim H and Kedward K T 2000 Modelling Hail Ice Impact and Predicting Impact Damage Initiation in Composite Structures *AIAA Journal* **38** 1278-88

[74] Juntikka R and Olsson R 2009 Experimental and modelling study of hail impact on composite plates *ICCM 17 (Edinburgh, 2009)*

[75] Perna-Sancher J, Pedroche D A, Varas J, jnr. Lopez-Puente and Zaera R 2012 Numerical modelling of ice behaviour under high velocity impacts *International Journal of Solids and Structures* **49** 1919-27

[76] Tippmann J D 2011 Development of a Strain Rate Sensitive Ice Material Model for Hail Ice Impact Simulation *(Masters Thesis)Univeristy of California, San Diego*

[77] Livermore Software Technology Company, 2013. [Online]. Available: http://www.lstc.com/corporate/profile.

[78] Keegan M H, Nash D and Stack M 2013 Numerical modelling of hailstone impact on the leading edge of a wind turbine blade *EWEA (Vienna, 2013)*

[79] Anghileri M, Castelleti L M L, Invernizzi F and Mascheroni M 2005A survey of numerical models for hail impact analysis using explicit finite element codes *International Journal of Impact Engineering* **31** 929-44

[80] Prayogo G, Homma H, Soemardi T P and Danardono A S 2011 Impact fatigue damage of GFRP materials due to repeated raindrop collisions *Transactions of the Indian Institute of Metals* **64** 501-6

[81] Zhou G 1996 Effect of impact damage on residual compressive strength of glass-fibre reinforce polyester (GFRP) laminates *Composite Structures* **35** 171-81

[82] Yuanjian T and Isaac D H 2008 Combined impcact and fatigue of glass fiber reinforced composites *Composites: Part B* **39** 505-12

[83] Kang K W, Kim J K and Kim H S 2005 Fatigue behaviour of impacted plain-weave glass/epoxy composites under tensile fatigue loading *Key Engineering Materials* **Vols. 297-300** 1291-6

[84] BladeCleaning 2013 BladeCleaning [Online]. Available: http://www.bladecleaning.com/. [Accessed 2013].

[85] Kumar V S, Vasa N J and Sarathi R 2012 Detecting salt deposition on a wind turbine blade using laser induced breakdown spectroscopy technique *Applied Physics A* 10.1007/s00339-012-7219-5

[86] Naka T, Vasa N J, Yokoyama S, Wada A and Arinaga S 2006 Experimental studies of lightning protection design for wind turbine blades *European Wind Energy Conference (Athens, 2006)*

[87] The Engineering Tool Box 2013 Salinity of Water [Online]. Available: http://www.engineeringtoolbox.com/water-salinity-d_1251.html. [Accessed 2013].

[88] Takaffoli M and Papini M 2012 Numerical simulation of solid particle impacts on Al6061-T6 Part II: Materials emoval mechanisms for impact of multiple angular particles *Wear* **296** 648-55

[89] Phan P T S andHuang S C 2008 Analysis of material loss from brittle erosion *Journal of Engineering Technology and Education* **5** 141-55

[90] Balu P, Kong F, Hamid S and Kovacevic R 2013 Finite element modeling of solid particle erosion in AISI 4140 steel and nickel-tungsten carbide composite material produced by the laser-based powder deposition process *Tribology Internationl* **62** 18-28

[91] Aquaro D 2006 Erosion rate of stainless steel due to the impact of solid particles *International Conference on Tribology (Parma, 2006)*

[92] El Togby M S, Ng E and Elbestawi M A 2005 Finite element modeling of erosive wear *International Journal of Machine Tools & Manufacture* **45** 1337-46